FOREWORD

This report was prepared by Arthur D. Little, Inc., under USAF Contract No. AF 33(616)-7472. This contract was initiated under Project No. 7350, "Ceramic and Cermet Materials Development", Task No. 735001, "Non-Graphitic". The work was administered under the direction of the Metals and Ceramics Laboratory, Directorate of Materials and Processes, Aeronautical Systems Division, with Mr. Fred W. Vahldiek acting as project engineer.

This report covers work conducted from July 1960 to December 1961.

Portions of the work reported herein were carried out under subcontracts with Arthur D. Little, Inc., as acknowledged in the text.

ABSTRACT

This report summarizes an integrated program of studies developed to provide thermodynamic and kinetic knowledge needed to describe the chemical behavior of zirconium and hafnium carbides and borides at temperatures to 3000K and in atmospheres of O_2, $O_2 + H_2O$, Cl_2, HF, F_2, H_2, CO, NH_3, and N_2.

The program consists of both internal and subcontracted efforts which can (1) provide, through calorimetric measurements, additional thermodynamic data needed for the tabulation of free energy functions of the zirconium and hafnium carbides and borides; (2) identify, by mass spectrometric means, gaseous species formed on vaporization of these carbides and borides and on their interaction with the several atmospheres; (3) provide thermodynamic data for important gaseous species through electron diffraction techniques, "matrix isolation" spectroscopy, and equilibria studies; and (4) develop the kinetics of the reactions of the carbides and borides with the various atmospheres through studies of the over-all rates of reactions and mass transport mechanisms. The status of each investigation is discussed in detail.

The preparation and characterization of macrocrystalline, high purity ZrB_2 and ZrC are described. Low temperature heat capacity data for ZrB_2 and heat content data for ZrB_2, ZrC, and HfB_2 are presented. The results of a study of the vaporization of ZrB_2 are reported.

PUBLICATION REVIEW

This report has been reviewed and is approved.

FOR THE COMMANDER:

W. G. RAMKE
Chief, Ceramics and Graphite Branch
Metals and Ceramics Laboratory
Directorate of Materials and Processes

TABLE OF CONTENTS

TABLE OF CONTENTS (Continued)

LIST OF FIGURES

LIST OF TABLES

I. INTRODUCTION

A. THE MATERIALS PROBLEM

There is an increasing demand in our technology today for structural materials to withstand high temperatures, steep temperature gradients, and corrosive atmospheres. The zirconium and hafnium carbides and diborides are among the highest melting materials known. The consideration of these materials for specific engineering applications can be simplified if we have the fundamental thermodynamic and kinetic knowledge which permits the predictions of their chemical behavior.

For a theoretical evaluation of the chemical behavior of a given ceramic material at high temperatures and under unusual atmospheric conditions, basic scientific information from several diverse studies must be integrated. In order to calculate the equilibrium condition for a given system, one must recognize the gaseous species which may be formed in the chemical interaction and must have thermochemical data on both the condensed and gaseous materials. In addition, to fully evaluate the usefulness of the ceramic material one must know something about the kinetics of the gas-solid interaction in order to determine whether equilibrium will be attained. Under some temperature conditions, knowledge of vaporization processes can be important.

Basic thermochemical and kinetic knowledge can also provide guidance for future materials development programs. For example, during the interaction of solids with gases surface films sometimes form which inhibit continuation of the reaction. As our understanding of the kinetic mechanism is improved, it is conceivable that we can design materials to favor the formation of surface films which will protect materials in high temperature applications.

B. THE TECHNICAL PROGRAM

Our program was initiated based on the current experience of some of our staff members in the pertinent scientific areas, the assistance of others, such as AVCO Corporation which was currently making a literature review of which a part was pertinent to our program, and the helpfulness of subcontractors and others with whom we talked. By these means we were able to select appropriate areas of study without having detailed the total program that will be required to obtain all desirable information. We have since developed a bibliography of studies related to the objectives of this program. The information derived from the literature search has modified the program slightly and will be utilized in the future in guiding the program as it progresses.

The program which has evolved includes calorimetric, mass spectrometric, spectroscopic, electron diffraction, equilibria, chemical rate, and mass transport studies. On the basis of our own experience and that of our subcontractors, we very early determined that the procurement of high purity samples was a very critical part of the over-all program. Each area of the program is discussed separately below.

Manuscript released by the author January 1962 for publication as an ASD Technical Documentary Report.

1. Sample Procurement

The basic value of much of the experimental work of the program depends on the providing of high purity samples. Samples of hafnium metal, hafnium carbide, hafnium diboride, zirconium carbide, and zirconium diboride of 99.9% purity or greater are required for calorimetric studies. These compounds should be macrocrystalline materials such as are obtained from a fusion process. They should be stoichiometric if possible. About 200 gm quantities of each material are required for low temperature heat capacity studies. The same material may be utilized later for other studies which require smaller quantities but which are more destructive of the sample material.

For kinetic studies we need dense, nonporous samples of zirconium and hafnium carbide and borides. These samples can be cut from fused buttons or single crystals. The effect of stoichiometry and trace impurities on the kinetic studies are expected to be important.

Since no commercial materials were available meeting our requirements, we initiated a program in our Cambridge laboratories, under the direction of George Feick, directed toward preparing and purifying commercial materials by means of a zone-refining technique.

2. Calorimetry

We are attempting to obtain the thermodynamic data for zirconium and hafnium monocarbides and diborides necessary to tabulate free energy of formation or free energy function vs. temperature for each compound. Thus, we require low temperature heat capacity measurements, high temperature heat content studies, and heat of formation determinations.

A knowledge of heat capacities to low temperatures permits calculation of entropies at 298K. For our purposes, the entropies of both compounds and elements are required. In addition, the calorimetric technique used in these heat capacity determinations provides highly accurate heat capacity data at room temperatures and slightly above, in which range heat content studies by the dropping calorimeter technique provide data of relatively high uncertainty.

Dr. E. F. Westrum, Jr., University of Michigan, accepted a contract to carry out low temperature heat capacity measurements of high purity macrocrystalline materials over the temperature range of 4-350K. He will study pure hafnium metal in addition to the carbides and borides of zirconium and hafnium. The best hafnium samples studied previously contained approximately 2% of zirconium. Furthermore, the data on the impure sample did not exceed 200K. These studies are proceeding as rapidly as high purity samples are available.

From heat content measurements, one computes free energy functions, $S_t - S_{298}$, $H_t - H_{298}$, and C_p at various temperatures. Once again, data for both the elements and the compounds are required by our program.

Dr. John L. Margrave, University of Wisconsin, is responsible for these measurements under a subcontract. One of the aims of his program is to develop techniques for heat content measurements to temperatures of 2200K. Conventional drop calorimetry has been used only to 1800K.

Accurate heats of formation of the carbides and borides are required. Some data have been reported previously for carbides from combustion bomb calorimetric studies carried out with an oxygen atmosphere. They were determined, however, on low purity samples. It is desirable to redetermine such data as higher purity samples become available. We have found that a common interest in obtaining the heat of formation data exists within other current programs in this country.

Dr. K. K. Kelley, U. S. Bureau of Mines, as a portion of an independent Bureau program has responsibility for the determination of heats of formation of carbides. He has indicated an interest in repeating measurements on the carbides if we can supply much higher purity materials than were previously available to him.

Oxygen bomb calorimetric technique has not been successful in determining reliable values for the borides because of the uncertainty in the final state of the boric oxide in the combustion reaction. Dr. Ward Hubbard, at Argonne National Laboratory, has recently developed a combustion bomb calorimetry technique using a fluorine atmosphere. Under these calorimetric conditions, the final states of the products are known without question. He has reported the heat of formation of ZrF_4 and BF_3. Thus, data is available for calculation of the heat of formation of ZrB_2 when its heat of combustion in a fluorine atmosphere is determined. Dr. Hubbard is interested in the studies of the borides as a part of his own program, and we have recently supplied him with high purity zirconium diboride prepared under this program.

3. Mass Spectrometry

Knowledge of gaseous species formed during vaporization or decomposition of the refractories and during the reaction of the refractories with various atmospheres is essential in order to select gaseous species for thermodynamic studies and in order to interpret kinetic data. The outstanding tool for such studies is the mass spectrometer. In addition to species identification, the mass spectrometer can provide thermodynamic data such as heats of sublimation and absolute vapor pressures.

Funds were provided by the Advanced Research Projects Administration for installation of a high temperature mass spectrometer in our Cambridge laboratories. This instrument was constructed by Nuclide Analysis Associates and is based on the Inghram design. Time has been made available on this instrument for studies of interest in this program. The studies are under the immediate direction of Dr. Alfred Buchler. Studies utilizing the mass spectrometer are of two types. In the first the problem is primarily one of studying the vaporization or decomposition of a refractory material. Initial efforts in this area consist in studies of the vaporization processes of the carbides and borides of zirconium and hafnium. This work can be carried out with the use of a simple effusion cell. The second type of study is concerned with the identification of gaseous products formed by the interaction of refractory material with a gas. For these studies a flow cell is required. This flow system permits the sampling of a gas stream after it has reacted with the refractory sample, so that a molecular beam representative of the product gas and containing the reaction products can be introduced into the mass spectrometer. Our initial studies are concerned with the zirconium oxide-water vapor system. Here our principal interest is in determining stability of gaseous zirconium hydroxides.

4. Spectroscopy

When the electronic, vibrational, and rotational spectra of gaseous species are known accurate data on entropy and heat capacity of the species can be obtained through statistical thermodynamic calculations. However, spectroscopy of gaseous molecules at high temperatures is extremely difficult. A potentially rewarding method for the spectral study of high temperature gaseous species is that of trapping individual gaseous molecules in a matrix of inert material.

Professor Otto Schnepp, Israel Institute of Technology, has undertaken, under subcontract, to prove the feasibility of the technique and to apply it to gaseous hafnium and zirconium species such as HfO and ZrO. These species are of interest, since they have been reported as primary gaseous species over the oxides. We might expect these oxides in systems where carbides or borides are reacting with oxygen or oxygen plus water.

In developing this technique, it is important to first investigate a series of substances whose vapor spectra are known, so that the results obtained from the matrix isolation technique can be compared and the matrix perturbation can be investigated. For this reason, initial work has been on the alkali halides. These studies will be followed by those on the zirconium and hafnium monoxides.

5. Electron Diffraction Studies

Rotational fine structure data necessary for statistical thermodynamic calculations are generally not obtainable from infrared spectra. Spectral studies in the microwave region are required. However, the rotational contributions to the partition functions for gaseous species can be computed when the molecular dimensions are known. Electron diffraction studies of gases can provide such data. Dr. S. H. Bauer has been pioneering in the application of electron diffraction techniques to high temperature gaseous species.

Professors S. H. Bauer and R. F. Porter, Cornell University, expect to obtain, under subcontract, electron diffraction data on the vapors of ZrF_4, $HfCl_4$, and HfF_4, and to establish their structures. It is now believed that the structure of $ZrCl_4$ is well enough established so as not to warrant further study at this time. Infrared spectra of the vapor at high temperature for these compounds are already available.

6. Equilibria Studies

When carbides and borides react with halogen containing atmospheres we can expect the formation of some gaseous subhalides of zirconium and hafnium as well as a formation of tetrahalide. In actual fact, subhalides may be more important at high temperature than the tetrahalides.

Dr. Freeman has undertaken a general program to determine chemical thermodynamic data for the subhalides of zirconium and hafnium. Initial emphasis will be on the di- and tri-fluorides and di- and tri-chlorides of zirconium because heats of formation and standard entropies at 298K are now available for ZrF_4 and $ZrCl_4$. The disproportionation equilibria of the lower fluorides and chlorides are to be studied initially with an absolute electrodynamometer momentum detector

which has recently been contructed in Dr. Freeman's laboratory. Various other techniques will be utilized as necessary for studying these equilibria.

7. Kinetic Studies

A knowledge of the kinetics of reaction of materials with various atmospheres is essential to complement thermodynamic calculations as it permits one to assess whether thermodynamic equilibria will be achieved for specific applications.

In general, gas-solid reactions are complex, i.e., the mechanisms consist of more than one step. Surface films are frequently formed, and diffusion of species through such films to the surface at which the reaction occurs must be considered. A detailed consideration of the mechanism may require knowledge of diffusion rates, solubility of gas in solid or solid in solid (i.e., phase diagrams for systems concerned are desirable), as well as over-all reaction rates.

One of the few kinetic studies on compounds such as carbides and borides has been the work of Dr. Joan Berkowitz-Mattuck in our Cambridge laboratories on the reactions of silicides, carbides, and nitrides in atmospheres containing controlled amounts of water and oxygen at temperatures to 2000C. During the period covered by this report, her work has been carried out under separate WADD contract.

Dr. John L. Margrave, University of Wisconsin, has as a portion of his program the study of the kinetics of reaction of hafnium and zirconium carbides and borides with oxygen, fluorine, water, and mixtures of these gases. A weight-gain technique utilizing a microbalance will be used for these studies, and the dependence of reaction rates on the nature of the reacting gas, temperature, and pressure will be investigated.

A mass transport study has been outlined to supplement kinetic studies within this program and those under way by Dr. Joan Berkowitz-Mattuck. This study is concerned with diffusion of reacting species through oxide and nitride films which can form in the reaction of the borides or carbides with oxygen or nitrogen containing atmospheres. This diffusion process can constitute one step in the over-all rate process and may be the rate limiting step under some conditions.

In the remaining sections of this report each individual study is discussed separately by the principal investigator concerned.

II. SUMMARY

A. PURPOSE AND SCOPE

The purpose of this program is to obtain thermodynamic and kinetic knowledge which is necessary for theoretical considerations on the use of the zirconium and hafnium carbides and borides at temperatures to 3000K and in atmospheres of oxygen, oxygen plus water, chlorine, hydrogen fluoride, fluorine, hydrogen, carbon monoxide, ammonia, and nitrogen.

To achieve this purpose, a technical program has been developed which will (1) provide all additional thermodynamic data on the carbides and borides of zirconium and hafnium necessary for tabulation of their free energy functions over a temperature range to 3000K; (2) identify gaseous species formed on vaporization of these carbides and borides or on their interaction with the several atmospheres of interest; (3) provide thermodynamic data for important gaseous species; (4) develop an understanding of the kinetics of the reactions of the carbides and borides with the various atmospheres.

B. ACCOMPLISHMENTS

The program of internal and subcontracted efforts in chemical thermodynamics and kinetics was planned and initiated to provide information needed to supplement that available in the literature.

The problem of sample procurement and preparation for the various studies under this program was resolved in favor of a single effort to produce high purity, high density carbides and borides of zirconium and hafnium. Experimental techniques were developed which can produce the desired high purity, high density carbides and borides from a melt. Zirconium boride and zirconium carbide were produced by this technique. Starting materials were obtained for the production of the hafnium carbide and diboride.

The heat capacity of the zirconium diboride was measured over the low temperature range (5-350K) by adiabatic calorimetry and found to be of normal sigmoid shape. Measurements are in progress on zirconium carbide.

A sample of the high purity zirconium diboride prepared under this program was supplied to Dr. Ward Hubbard at Argonne National Laboratory. Dr. Hubbard's group at Argonne is interested within its own program in the heat of formation of compounds such as zirconium diboride. The compound will be studied by a fluorine combustion calorimetry technique developed at the Argonne National Laboratory.

Zirconium-free hafnium metal was sought for the purposes of materials preparation and calorimetric studies, but could not be located. However, we were offered the loan of a crystal bar sample containing 0.7% zirconium by the workers at Argonne National Laboratory. Professor Westrum has completed arrangements to obtain this material for the measurement of low temperature heat capacities. This measurement is nondestructive and the material can be returned.

Heat content data to 1200K are reported for zirconium diboride, hafnium diboride, and zirconium carbide. These data are from measurements made on powdered samples supplied Dr. John Margrave by The Carborundum Company. The study was initiated prior to the start of this program and was completed under this program. The results will be checked again and will be extended to higher temperatures on boride and carbide samples prepared within this program. Modifications to the heat content calorimeter were initiated which will permit the extension of measurements to 2200K.

Mass spectrometry studies are being used to obtain information on the vaporization and dissociation processes of the carbides and borides as well as a tool for the study of the kinetics of gas-solid reactions. The results of a study of the vaporization of zirconium diboride are reported. The status of the development of a flow system for the kinetic studies on gas-solid reactions, together with the initial test work, are discussed.

To provide spectral data permitting the calculation of thermodynamic functions by the methods of statistical mechanics, studies on the spectroscopy of high temperature gaseous species such as ZrO and HfO by matrix isolation methods were initiated. Current efforts are directed toward resolving the question of the perturbation effect of the matrix on the trapped molecule. Toward this end it is important to first investigate a series of substances whose vapor spectra are known so that the results obtained can be compared and the matrix effects determined. The alkali halides are under study and spectral data are presented for the case of lithium chloride.

Studies to obtain electron diffraction data on the vapors of zirconium tetrafluoride, hafnium tetrachloride, and hafnium tetrafluoride and to establish their structures were initiated. The data obtained will permit calculation of statistical thermodynamic properties of the gaseous tetrahalides.

An evaluation of various thermodynamic properties of the zirconium and hafnium subhalides through a study of disproportionation equilibria was initiated. Accomplishments to date include development of a suitable momentum measuring device and theoretical study of the correction factors for both total flow and angular distribution of molecules effusing from conical orifices.

Under the direction of Dr. John Margrave, studies on the kinetics of reaction of hafnium and zirconium compounds with oxygen, water, and fluorine and with mixtures of these gases are under way. A quartz helix microbalance was incorporated in a glass metal vacuum system suitable for use with chlorine as a reactant. Calibration of this device by oxidation of various pure metals in oxygen is in progress.

A mass transport study was developed to supplement kinetic studies within this program. Experimental techniques were outlined and equipment procured for the measurement of oxygen diffusion in zirconium oxide. Experiments on single crystal samples of ZrO_2 appear most desirable. Current experimental efforts are directed towards growing single crystals by hydrothermal techniques.

C. PLANS FOR FUTURE WORK

During the coming year, a program on oxidation of refractory materials now under way in our Cambridge laboratories under the direction of Dr. Joan Berkowitz-Mattuck will be incorporated within this program. Her studies will provide information on the kinetics of oxidation of the borides and carbides of zirconium and hafnium. The other portions of our program, which are described in this report, will be continued throughout the next year.

We anticipate that by the end of the next year sufficient thermodynamic data will be available to permit the tabulation of the free energy function for the carbides and borides of zirconium and hafnium to temperatures of 2200K, and extrapolation beyond that to 3000K. The kinetic studies now underway should provide by the end of the year knowledge concerning the reactions of the carbides and borides with atmospheres of oxygen, fluorine, hydrogen fluoride, water, and mixtures of these gases. We expect that thermodynamic studies will be completed for the tetrahalides and monoxides of zirconium and hafnium.

For the next year approximately three fifths of our total effort is concerned with questions relating to the kinetics of the reactions of carbides and borides with the atmospheres of interest. Approximately one fifth of our program is directed towards completing the thermodynamic studies on the solid carbides and borides and the remaining one fifth of the total program is concerned with providing thermodynamic data on gaseous species produced in the reactions of these borides and carbides with the various atmospheres. These latter studies include the spectroscopy, electron diffraction, and equilibria studies on the halides and oxides of zirconium and hafnium.

III. SAMPLE PROCUREMENT AND PRODUCTION*

During this report period, we have substantially completed our procurement of samples of pure ZrB_2, ZrC, HfB_2, and HfC to be used as starting materials for zone refining. Arrangements have been made for the loan of a sample of hafnium metal for low temperature heat capacity measurements. Details of the procurement problem are discussed in Section A below.

The production and characterization of 200 gm of zone-refined zirconium diboride have been completed. Samples have been furnished to Professor E. F. Westrum, Professor J. L. Margrave, Dr. W. N. Hubbard, and Dr. Alfred Buchler for thermodynamic and kinetic studies. Something over 100 gm of this material is still available for future needs.

Considerable difficulty has been encountered in zone refining zirconium carbide and in controlling its stoichiometry. These problems now appear to have been solved and the production of 200 gm of zone-refined material is nearly complete. The acceptability of this lot of material will be finally determined by analyses now in progress.

Preliminary experiments with hafnium carbide indicate that this material is quite difficult to melt by induction heating. Partial melting has been achieved in several experiments, however, and we have reasonable expectations of being able to zone melt this material.

Details of the experimental work are given in Section B below.

A. PROCUREMENT OF RAW MATERIALS

1. Zirconium Diboride

We obtained samples of ZrB_2 in the form of fine powders from U. S. Borax Co., Norton Co., and H. C. Starck (Göslar, Germany). Semiquantitative spectroscopic analyses indicated that the hafnium content of all these samples was in the range of 0.01% to 0.1%. Other metallic impurities were in the same general range or less. The Norton sample was lower in molybdenum than the other two, although silicon, calcium, and aluminum were higher. We originally reported that all these materials were considered satisfactory for sample preparation, and the U. S. Borax product was selected for initial experiments.

However, we later found that routine spectrographic analysis for hafnium in these materials is not reliable. Samples that were reported by several spectrographic laboratories to contain less than 0.1% Hf were found by X-ray fluorescence analysis to contain several percent of hafnium. For this reason none of the early commercial samples obtained was suitable for use.

---

* - Submitted by George Feick, Arthur D. Little, Inc., Cambridge, Mass.

Further inquiries indicated that The Carborundum Company was willing to produce on special order a sample of ZrB_2 from nuclear-reactor grade zirconium. We ordered and received two pounds of this material. The analysis as reported by The Carborundum Company is as follows:

Zirconium	77.25%
Boron	19.58
Oxygen	.2
Total Carbon	0.57

Spectrographic Analysis:

Al	.01-.05 %
Ca	.01-.05
Cr	.01-.05
Cu	.005-.01
Fe	.01-.05
Hf	.001-.005
Mn	.05-.1
Ni	.01-.05
Si	.01-.05
Ti	.005-.01

We confirmed by X-ray fluorescence analysis that the hafnium content of this sample is below the limit of detection of our apparatus, which is about 0.1%.

The above data indicate a B:Zr ratio of 2.104, about 5% in excess of the stoichiometric requirements. No attempt was made to correct the stoichiometry of the sample since some boron is lost by sublimation during zone refining and an excess is expected to be largely self-correcting.

2. Zirconium Carbide

A sample of ZrC in the form of fine powder from H. C. Starck was found by spectrographic analysis to contain from 0.01% to 0.1% Hf and minor amounts of other metals. We originally reported that we considered this material satisfactory for further purification. However, the experience discussed above with zirconium diboride led us to suspect the reliability of this value. We analyzed this sample, therefore, by the X-ray fluorescence method, which indicated that it contained about 1.7% of hafnium and was undesirable for our purposes.

We obtained, therefore, from The Carborundum Company, two lots of ZrC made from nuclear-reactor grade materials. The first lot of two pounds was largely consumed in preliminary experiments with sintering methods. Attempts to extend the supply with ZrC made from the elements were unsuccessful because of the difficulty of controlling stoichiometry.

The second lot of ZrC (four pounds) is being used in current production. The following analysis of this lot is furnished by the supplier:

Chemical Analysis:

Zr	88.16%
C (total)	11.45
O_2	.05
N_2	.15
Fe	.12

Spectrographic Analysis:

Ag	.0002%
Al, Ca, Co, Mo	.001 to .005
Mg, Sn, Pb	.005 to .01
Sb, Ti, Si	.01 to .05
Cu, Mn, Ni, B	.05 to 0.1

The carbon content of this material is somewhat below theoretical (11.63% C) and is further reduced during zone refining by reaction with oxygen. Two zone-refined bars from the above lot gave 10.80% C and 10.88% C on analysis. In producing the final lot of material, therefore, we have added the calculated amount of pure graphite to the starting material in order to bring the carbon content up to the theoretical value.

We have obtained independent spectrographic analyses on the ZrC as received from The Carborundum Company and on one of the zone refined bars. The results indicate that boron and titanium may be somewhat higher than reported by the supplier. Further analytical work will be needed to resolve this discrepancy.

3. Hafnium Metal

Although hafnium-free zirconium is readily available, the same is not true of zirconium-free hafnium. Pure metallic hafnium is desired for heat capacity measurements and for conversion into the boride and carbide. For heat capacity measurements we desire a zirconium-free material of high purity which has been subjected to refining steps such as the "iodide process" or electron beam melting. Extensive inquiries failed to disclose a source of hafnium containing less than 1.1% of zirconium. The material containing 1.1% zirconium was sponge material, not refined metal, available from The Carborundum Company. Wah Chang Corporation produces some of the purest hafnium available on the market by electron beam melting of sponge metal, but it contains approximately 2.5% zirconium. It now appears that zirconium-free hafnium metal would have to be made on special order. We have neither time nor funds on the present project to cover this procurement. We have been offered, however, the loan of a small quantity of crystal bar hafnium metal containing 0.7% zirconium for the nondestructive low temperature heat capacity measurements. Arrangements are being made to accept this kind offer.

4. Hafnium Diboride

The Carborundum Company offers a grade of HfB_2 containing about 6000 ppm of Zr, which appears to be the purest material available commercially. We have

ordered three pounds of this material and expect delivery about November 21, 1961.

If a purer material is desired in the future, it could probably be made by reacting pure HfO_2 containing about 175 ppm Zr (from Wah Chang Corporation) with pure boron carbide.

5. Hafnium Carbide

We have obtained 3.5 lb of HfO_2 containing an average of 340 ppm of Zr from Wah Chang Corporation. The Carborundum Company will convert this into hafnium carbide on a toll basis. We expect delivery about November 15, 1961.

B. PRODUCTION OF ZONE-REFINED BARS

The production of zone-refined refractory materials suitable for thermodynamic and kinetic measurements involves three major steps:

1. Preparation of sintered feed rods
2. Zone refining
3. Selection and characterization of the product.

These steps are discussed in detail below.

1. Preparation of Sintered Feed Rods

The zone-refining apparatus is designed to use rods 1/4 to 1/2 inch in diameter by 8 to 10 inches long. The fabrication of these brittle materials into bars of such large length-to-diameter ratio offers considerable difficulty.

The nature of these refractory powders is such that any cold pressing or extrusion operation requires the use of binders to give the rods enough strength to permit handling. To avoid the introduction of unnecessary impurities, we decided to fabricate the required bars by high temperature sintering at moderate pressure without the addition of extraneous binders.

Successful sintering methods have been developed both for zirconium diboride and for zirconium carbide. Because the processes used for the two materials differ in detail, they will be discussed separately.

(a) Sintering of Zirconium Diboride

The first problem to be faced in developing a sintering method for ZrB_2 was the choice of a suitable mold material. Alumina and graphite were rejected because of the possibility of contaminating the product. Zirconia and boron nitride were considered suitable from this standpoint, and the latter material was chosen because of its easy machinability. The molds were fabricated from boron nitride rods 8 inches long by 3/4 inch diameter by drilling a 3/8 inch hole through the center of the rods, splitting the resulting tube longitudinally into two halves with a thin milling cutter, and reaming to 3/8 inch diameter.

It was found that the resulting molds were almost entirely inert toward heated ZrB_2 and were reasonably durable except that the boron nitride showed a tendency to soften and bend at the sintering temperatures used. This bending was prevented by enclosing the boron nitride mold in a split alumina tube which was sufficiently rigid at high temperature to hold the boron nitride straight. The mold assembly was held together by binding with tantalum wire.

After the mold was packed with powdered ZrB_2, short electrodes were inserted in each end of the mold and the assembly was clamped between heavy copper electrodes in a vacuum chamber and heated by the passage of a heavy current. The electrodes were either graphite or preferably pieces of previously sintered ZrB_2 rod in order to minimize contamination.

This electrical heating has the advantages that the heat is applied directly to the sample and that the heating time is short. Thus, reaction of the ZrB_2 with the mold is practically eliminated.

The chief difficulty encountered with the above sintering method was the large change in resistance of the sample as the sintering progressed. The initial resistance of the powdered ZrB_2 packed in the mold was of the order of 1,000 megohms, while the final resistance of the sintered bar was about 1/40 ohm. This large change necessitated the use of a series of power supplies during sintering in order to match the impedance of the sample well enough to heat it effectively.

Because of the high initial resistance of the sample, we were unable to pass enough current through it at readily available voltages to raise its temperature appreciably. This problem was solved by surrounding the filled mold with an auxiliary heating element made of an alumina core wound with nichrome wire. It was found that when the mold temperature was raised to 300-400C by means of this auxiliary heating element, the resistance of the sample fell to something of the order of several hundred ohms, probably because thermal expansion forced the boride particles into closer contact.

At this point the application of 115 volts caused enough current to flow to heat the sample rapidly with an accompanying sudden decrease in resistance to about 1 ohm. Current flow was limited, therefore, to 15 amperes by means of a series resistance.

The power supply was then switched to a variable transformer (Variac) and a current of 40 amperes maintained through the sample for about 1 minute. During this period, the resistance of the sample continued to drop and the voltage was decreased in order to maintain constant current.

When the resistance of the sample reached about 0.3 ohm, a high-current transformer was connected and sintering was continued at an applied potential of about 10 volts for about 15 minutes. Final sintering was accomplished by holding a constant current of 400 amperes at about 10 volts through the sample for about 1 minute. At the end of that time, the sample temperature was estimated to be over 1500C.

Figure 1 shows a photograph of the sintering apparatus. The bell jar contains the mold and the auxiliary heater which is visible in the picture. In use, a stainless-steel radiation shield surrounds and conceals the auxiliary heater. A disassembled mold and a sintered bar are on the table to the left of the bell jar. The electrical components necessary for supplying the various voltages and currents are mounted below the table.

Control of the particle size of the ZrB_2 is important. We found that finely powdered ZrB_2 (5-10 micron) gave low density bars which were difficult to zone refine. If the ZrB_2 were crushed only enough to pass a 30 mesh screen, a density of about 62% of theoretical was obtained, which was found satisfactory for zone refining.

With a material of 30 mesh particle size, however, we found that the strength of the sintered bars was so low as to cause trouble with breakage in handling. The trouble was overcome by adding 2 grams of a stoichiometric mixture of reactor-grade zirconium hydride (Metal Hydrides, Inc.) with 99.1% boron (U. S. Borax and Chemical Corp.) to every 100 grams of zirconium boride. During sintering, this mixture reacted to form additional ZrB_2, thus functioning as a bonding agent without introducing extraneous impurities. The bars produced from this mixture were strong enough for convenient handling and were used for the subsequent zone-refining operation.

(b) Sintering of Zirconium Carbide

Initial attempts to sinter zirconium carbide were made in the apparatus of Figure 1 using a mold of high purity graphite in place of boron nitride. We were unable to make coherent bars by this method even with the addition of about 20% of a sintering aid composed of a stoichiometric mixture of zirconium hydride with pure spectrographic graphite (United Carbon Products Co.) This difficulty appeared to be due in part to the more refractory nature of the carbide and in part to the fact that the heating current was no longer confined to the sample but flowed in part through the mold. The highest mold temperature attainable with our power supply was about 1200C as measured by optical pyrometer. It appeared that the sample was little if any hotter than this. (In the case of the boride in the boron nitride mold, the sample was much hotter than the mold and probably attained a temperature upwards of 1500C)

This problem was overcome by mounting the filled graphite mold in the zone-refining apparatus (see below for description) and using the 10 kw, 450 kc power supply for heating. By this means, a section of the mold about 1-1/2 inches long was heated to a surface temperature of 1850C as measured by optical pyrometer. The heated zone was moved over the length of the bar at a rate of 20 inches per hour while keeping the sample under slight compression. The bars so produced showed satisfactory strength and were used for zone-refining operations.

2. Zone Refining

The zone-refining apparatus used in this work was of the vertical, induction-heated, floating-zone type, operating in an inert gas at about 1 atm pressure. The presence of the atmosphere has been found necessary to prevent excessive evaporation of the molten zone at the high temperatures involved. Most of the samples have been

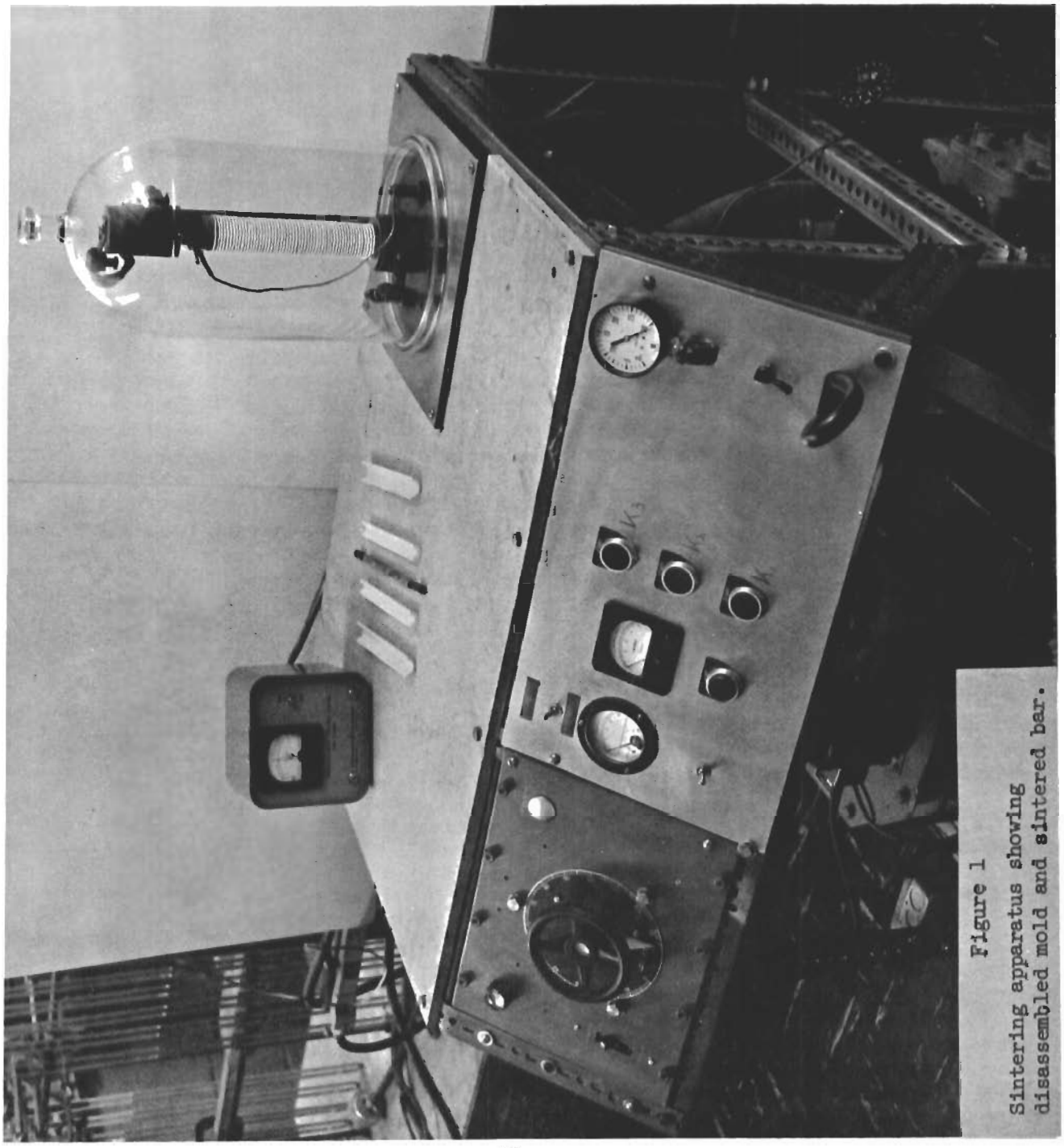

Figure 1
Sintering apparatus showing disassembled mold and sintered bar.

refined at 20 inches per hour using a 10 kw, 450 kc power supply. In some cases, improved crystal structure is obtained at speeds as low as one or two inches per hour. For very high melting materials such as HfC the use of a larger power supply may be necessary.

Figure 2 shows the working chamber of the zone refiner with the bell jar raised and a sintered rod of ZrB_2 in place in the sample holders. Figure 3 shows the appearance of a ZrB_2 bar after zone refining.

In essence, the operation of the zone-refining apparatus consists of regulating the power input to the molten zone in such a way as to keep the zone as small as possible while still maintaining it in a completely molten state. In our apparatus, this regulation requires the continuous attention of an operator who adjusts the power input and other variables in accordance with visual observations of the floating zone. In spite of this continuous attention, we find that the maintenance and control of the zone in refractory materials such as ZrB_2 and ZrC offers a number of experimental difficulties, most of which can be overcome by suitable choice of the variables at the control of the experimenter. Some of these difficulties and the means available for their correction are discussed below.

One of the most common problems is the overflowing of the molten zone, which blocks or disturbs the operation. These runovers are caused in part by gravity and in part by the repulsive force of the high frequency field. Occasionally a situation is encountered where the operating margin between incomplete melting and overflowing is very narrow and where runovers occur in spite of careful regulation. Under these conditions it may be necessary to alter the coil design so as to vary the levitating effect of the electric field. The speed and direction of zone travel also influence the ease of control and it is usually necessary to vary the operating conditions with a new material until a stable zone is obtained.

In some cases it has been found helpful to place gas jets, fed with argon, below the induction coil. The cooling effect produced by these jets tends to move the molten zone to a higher position with respect to the coil, thus increasing the benefit obtained by the levitating effect of the field.

If the sample is impure, the impurities will tend to build up in the floating zone, thus decreasing its melting point and increasing its size and its tendency to overflow. For this reason it is necessary to pay careful attention to the purity and stoichiometry of the raw materials.

A second difficulty, which appears to be especially severe with the carbides, is the nonuniform melting of the sintered rod ahead of the molten zone. This nonuniformity may take the form of a partial melting of the center of the rod, leaving a partial shell of solid material on the outside. This partial shell is a poor susceptor and cannot be melted at ordinary power levels with our power supply. In other cases the sintered rod may expand and bulge ahead of the moving coil. This swelling causes excessive arcing and leads to nonuniform heating. In extreme cases, the molten zone may be forced by the electric field into this swollen region even when it is above the coil, forming a kind of inverse runover.

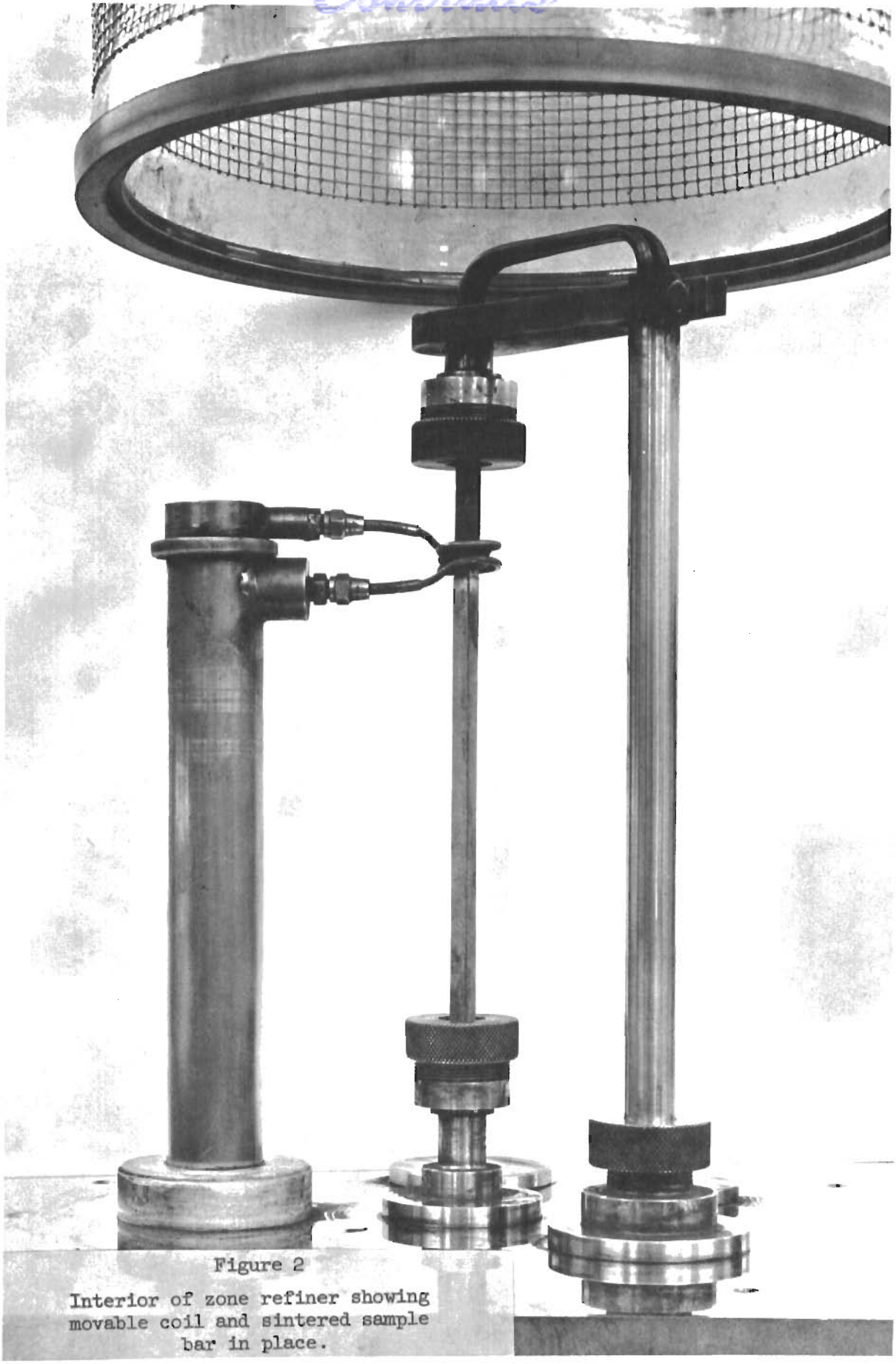

Figure 2

Interior of zone refiner showing movable coil and sintered sample bar in place.

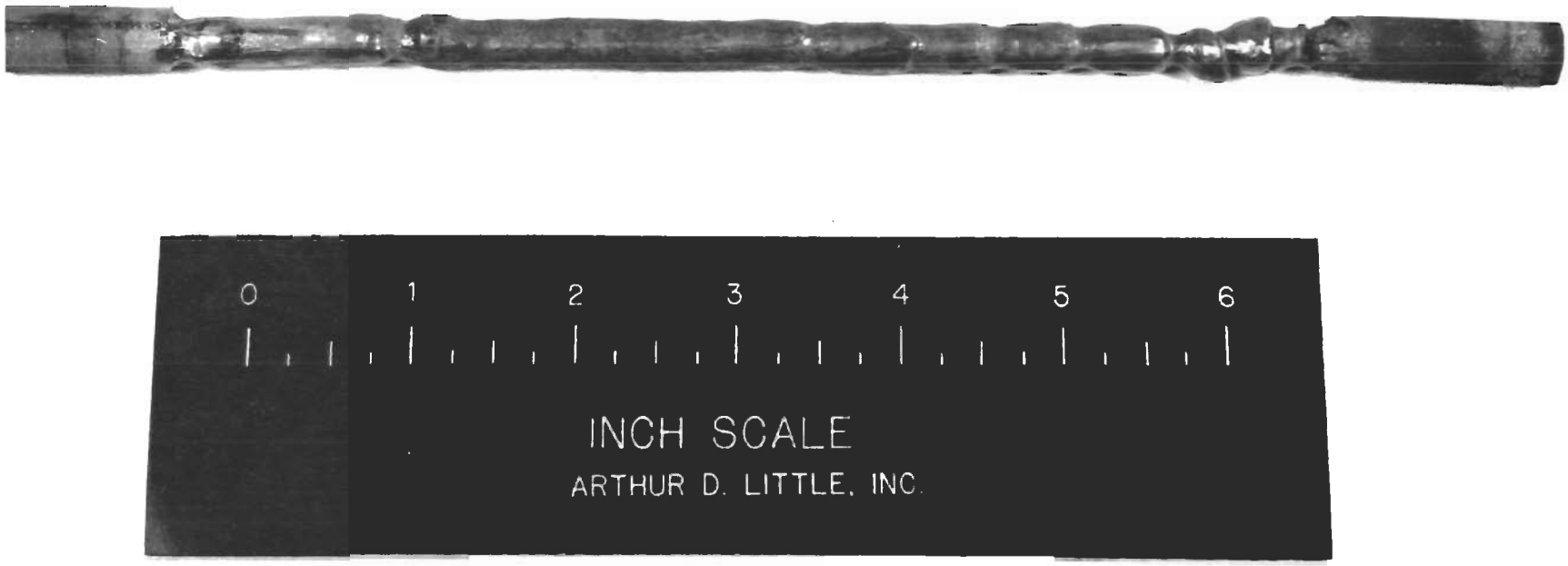

Figure 3

Typical zirconium diboride bar after zone refining.

Much of this nonuniform melting appears to be due to penetration of the molten zone by capillarity into the sintered bar. This can be controlled by reducing the porosity of the sintered bar (a theoretical density of 50 to 65% is satisfactory in most cases) and by employing gas jets to cool the sintered bar and limit liquid penetration.

Liquid penetration is increased also by impurities and probably by the presence of incompletely reacted raw materials in the sintered rod. It can be controlled to some extent by using pure, stoichiometric and completely reacted raw materials.

A third difficulty is the nonuniform solidification of the bar behind the molten zone. In extreme cases the zone-refined bar may have the appearance of a string of beads held together by narrow necks of material. Under these circumstances no control of the crystal structure nor of the separation of impurities is possible. The trouble appears to be aggravated by the fact that a narrow neck is a less effective susceptor than a larger section of the rod and the effective power supplied by the radio-frequency generator varies over a wide range.

This condition can be relieved to some degree by the same means used to control nonuniform melting due to liquid penetration. The use of gas-jet cooling is especially helpful. Variation of speed and direction of zone travel and changing the coil configuration may also be desirable.

A fourth source of difficulty is the arcing of the high frequency current from the coil to the rod. This is especially troublesome with high melting materials since it is necessary to use close-fitting coils and high power levels in order to melt the rod. Electron emission from the heated sample and the sublimation of materials on the coil also play a role in the initiation of arcing.

The occurrence of arcing disturbs the uniformity of the refining operation and in extreme cases may puncture the heating coil, allowing the cooling water to run into the working chamber. This problem has been largely overcome by the addition of hydrogen to the argon atmosphere of the zone refiner, in which it appears to exert a quenching effect on the arc discharge. In most cases about 5% of hydrogen in argon is sufficient, but some additional benefit is obtainable by using pure hydrogen. By using 5% hydrogen, we are now able to decrease the coil clearances sufficiently to refine zirconium carbide with the 10 kw power supply. This arrangement is being used in current production.

In spite of these difficulties, we have zone refined about 33 bars of zirconium diboride of which the first ten were preliminary runs made with material containing hafnium. Of the remaining 23 bars, sixteen have yielded material of satisfactory quality as judged by uniformity of dimensions and crystal structure. The 200 grams of zone-refined ZrB_2 sent to Professor Westrum, as well as a number of samples for chemical and metallographic analyses, have been selected from these bars. The selected regions are removed by diamond-sawing and cleaned of surface oxide by pickling in a mixture of nitric and hydrofluoric acid.

The yield of zirconium carbide has been considerably lower. To date we have made about 80 bars of this material of which the first 60 have been rejected because of difficulties in sintering, zone refining, or control of stoichiometry. These problems have now been solved, however, and the last 20 bars have yielded about 200 grams of material which will be acceptable if the chemical analysis proves satisfactory.

We have made 29 bars of hafnium carbide using starting material made by reaction of HfO_2 with carbon. None of these runs has been successful, because of poor sintering and of irregular melting. We expect that the new batch of hafnium carbide will behave considerably better, primarily because it will have been completely reacted prior to sintering.

3. Characterization of Products

Samples of the zone-refined products are being characterized by chemical and spectrographic analysis, by X-ray diffraction, and by metallographic methods. This work has been completed for zirconium diboride and partly completed for zirconium carbide. The results obtained to date are discussed below.

(a) Zirconium Diboride

Preliminary work has shown that powdered ZrB_2 may contain considerable oxygen in the form of zirconium oxide, which is almost completely removed on zone refining. A preliminary sample containing about 1.5% of ZrO_2 (estimated as an insoluble residue from solution of the sample in aqua regia) showed only 70 ppm of oxygen after zone refining as measured by an inert-gas fusion technique.

Two further samples of zone-refined ZrB_2 from the lot sent to Professor Westrum were analyzed by the same method by Ledoux and Co., Teaneck, New Jersey. One of these (composite of samples 80-3 and 80-5) was reported to contain 48 ppm of oxygen; the other (sample 81-5B) was reported to contain 56 ppm of oxygen. The latter sample contained a part of the final molten zone and should represent a concentrated sample of most of the impurities present. These values are considered satisfactorily low.

Two samples (83-4 and 87-4B taken from the final end of the bars, which is probably the worst case) were analyzed for zirconium and boron. The results as reported by Schwartzkopf Microanalytical Laboratory were:

	83-4			87-4B		
	1	2	ave.	1	2	ave.
Zr	80.05	79.60	79.82	80.74	80.40	80.57
B	18.70	18.90	18.80	18.98	19.09	19.04
TOTAL			98.62			99.61
B/Zr ratio			1.96			1.99

Three samples (81-1, 81-3, and 81-5A) representing the beginning, the middle, and the end of a single bar were reported by Ledoux and Co. to contain 260, 165, and 220 ppm of carbon respectively. This is considerably lower than the value of 0.57% carbon reported by The Carborundum Company for the raw material and independently checked by Ledoux and Co. This result indicates that considerable carbon has been removed during zone refining, probably in the form of carbon monoxide due to reaction with oxygen. Since there appears to be no significant trend in carbon content attributable to zone refining, an average value of 215 ppm carbon was taken as representative of this lot.

Four samples (82-1, 82-3, 82-4, 82-6) taken at various points along a single bar of ZrB_2 were submitted to Jarrell-Ash Co., Newtonville, Mass., for spectrographic analysis. It was reported that the material as received burned very unevenly in the arc and gave poor results. The samples were dissolved, therefore, in aqua regia and evaporated to dryness. The resulting salts could then be analyzed satisfactorily. The results showed that the zone-melting operation had produced a considerable reduction in trace metal impurities, apparently by evaporation from the molten zone. There was no systematic trend in any of the impurities over the length of the bar, an indication that no strong movement of any of the impurities had taken place during the single pass to which the specimen had been subjected. A typical analysis is given below:

Impurity	Amount Present (%)
Mg	.001 to .01
Al	.001 to .01
Si	.01 to .1
Cu	.001
Ti	.001
V	.001
Cr	.001
Mn	.001
Fe	.01
Cu	.001
Ag	.001
Hf	.01

Four samples (80-1, 80-6, 88, 100-2) from the same lot of ZrB_2 have been analyzed by X-ray diffraction. Of these, the last three represent portions of the molten zone after solidification, which we expected to contain a high concentration of impurities and, therefore, to permit a highly sensitive test. None of the samples showed any significant diffraction lines other than those reported for ZrB_2.

The metallographic structure of zone-refined ZrB_2 presents several points of theoretical and practical interest. The initial part of the bar appears polycrystalline in cross section and consists of columnar grains about a millimeter in cross section. After about an inch of zone travel, however, the number of crystals diminishes until the cross section contains from one to about three crystal grains. These grains are surrounded, however, by a polycrystalline surface layer about 1/2 mm thick which consists of long (1 to 5 centimeters) columnar grains arranged like the staves of a barrel. A typical ZrB_2 cross section is shown in Figure 4. The specimen was polished and etched for 30 sec with a mixture of 20 parts HNO_3, 20 parts HF, and 60 parts glycerol.

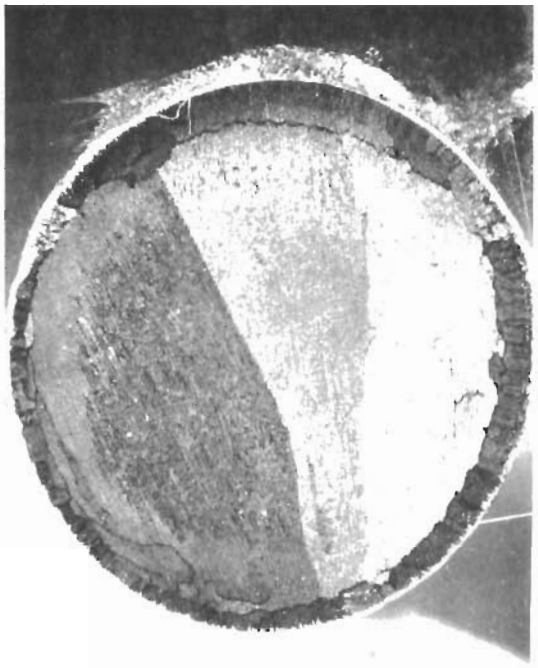

Figure 4

Zirconium Diboride
Cross section
10 X
Etched

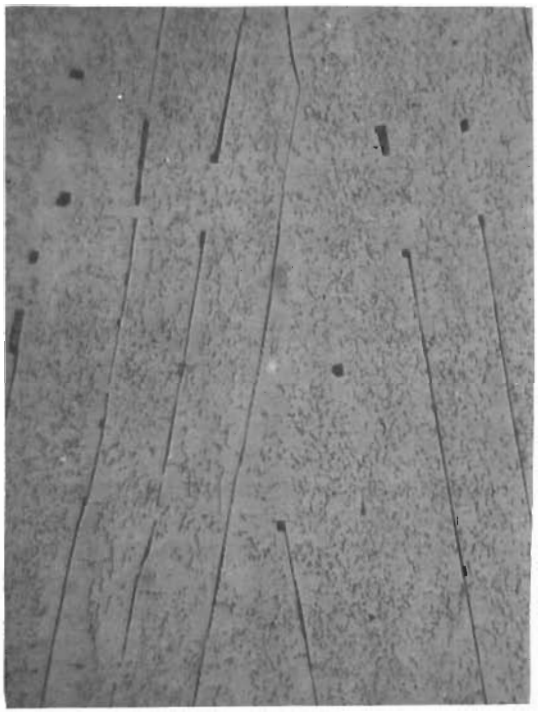

Figure 5

Zirconium Diboride
Cross section at grain boundary
200 X
Etched

It is apparent from Figure 4 that the three main crystal grains have a lamellar substructure. This substructure is shown at a higher magnification in the vicinity of a grain boundary in Figure 5. The lamellae appear to be caused by the inclusion in the cell boundaries of a very small amount of a second phase which breaks up into columnar structures of rectangular cross section in several places. In view of the slight boron deficiency shown by the chemical analysis, these inclusions are considered to be a zirconium-rich phase, possibly ZrB.

The fine structure between the lamellae of Figure 5 has been briefly examined by electron microscopy. It consists of oriented, V-shaped grooves running in two perpendicular directions. It seems likely that these grooves consist of etch pits which have been run together by overetching. If so, they indicate the presence of dislocations in the crystal which may have a profound effect on future kinetic studies.

The presence of a lamellar substructure in ZrB_2 indicates that our present rate of zone travel (20 inches per hour) is too fast to permit diffusion of impurity atoms ahead of the growing crystal front. Instead the impurities can diffuse only as far as the cell boundaries where they are incorporated in the crystal.

The amount of foreign material in the cell walls and in other inclusions does not appear to be large enough to have much effect on heat capacity measurements. In oxidation measurements and other corrosion studies, however, the cell walls may facilitate chemical attack in the same manner as intergranular impurities, thus exerting a profound influence on the experimental results. Since intergranular and intercellular impurities are in general expected to be lower melting than the pure materials, they will probably have a strong adverse effect on mechanical properties at high temperatures.

In view of these considerations, it appears highly desirable to study the nature of the cellular growth as functions of zone speed and number of passes. We plan to pursue this question to the extent that time and budget permit.

(b) Zirconium Carbide

Chemical analysis of the ZrC bars is still in progress. As stated in Section A-2 above, there appears to be a question about the boron and titanium content of the material.

We have made one bar from the first lot of ZrC, however, which is very nearly of stoichiometric composition (11.57% carbon vs. 11.63 theoretical). Spectrographic analysis of a similar bar shows negligible trace impurities.

A cross section of the bar (No. 114), polished and etched with diluted Tucker's etch (130 ml H_2O, 237 ml HCl, 83 ml HNO_3, and 50 ml HF) is shown in Figure 6. The vertical lines to the right of the cross section are the result of a fracture during the mounting of the specimen. A polycrystalline surface layer is also evident in this sample although the line of demarcation is less sharp than in the case of ZrB_2. A photograph of the central area of the bar at higher magnification is shown in Figure 7. A few grain boundaries are found, but no evidence of cellular structure or of etch pits.

Figure 6

Zirconium Carbide
Cross section
10 X
Etched

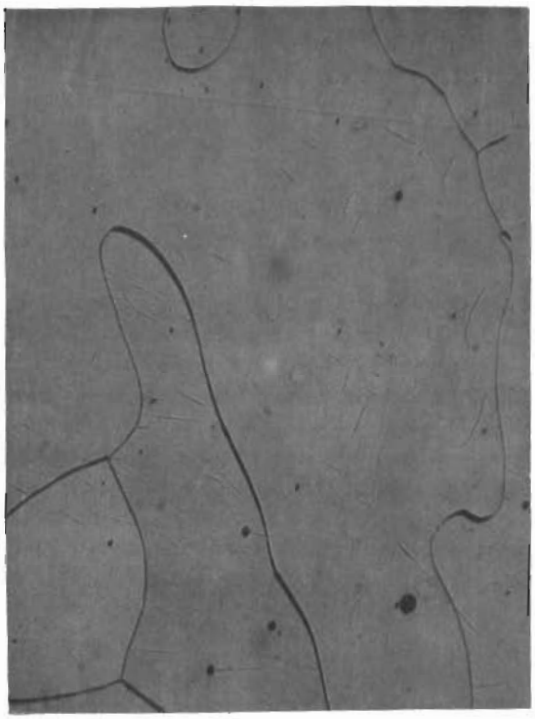

Figure 7

Zirconium Carbide
Cross section
50 X
Etched

A small excess of carbon results in the formation of a well-marked polygonal cell structure as shown in Figure 8. This bar (No. 110) contained 12.05% of carbon or a 3.6% excess based on the theoretical carbon content of 11.63%. The cell structure is evident in the unetched, polished specimen and is probably caused by the segregation of free graphite. In some cases the segregation of excess graphite in the grain boundaries of ZrC has resulted in the spontaneous disintegration of the zone-refined bars into their individual grains. The graphite in the grain boundaries is evidently unable to support the stresses arising from cooling the bar.

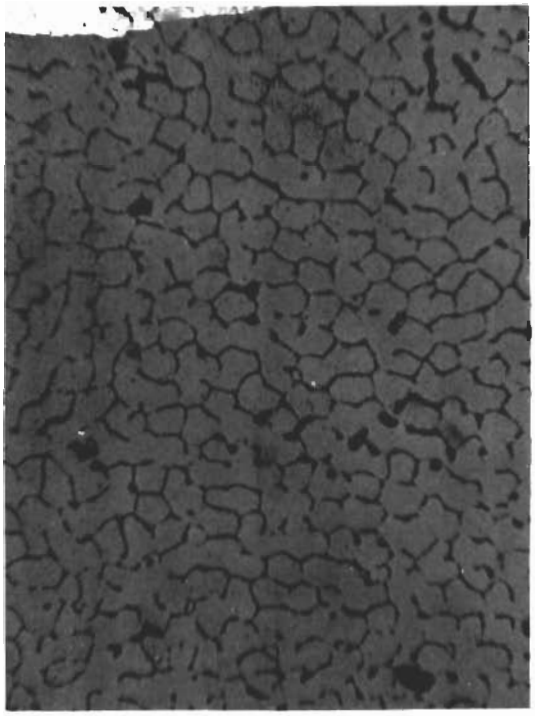

Figure 8

Zirconium Carbide
with excess carbon

Cross section

70 X

Not etched

IV. LOW TEMPERATURE HEAT CAPACITY MEASUREMENTS*

Accurate thermodynamic data on carbides, borides, and related compositions of the group IV elements are relatively rare. The major reason for this fact is the difficulty of preparing these substances in high purity, well-characterized states suitable for thermodynamic reference use. The present study represents an initial endeavor to procure reliable thermodynamic data on these materials by adiabatic calorimetry.

A. EXPERIMENTAL

1. Cryostat and Technique

Measurements were made in the Mark II adiabatic, vacuum cryostat schematically similar to one previously described,[1] but modified and improved in several respects to give an instrument of greater compactness, mechanical rigidity, and operating convenience. The cryostat is provided with an "economizer" which is essentially a heat exchanger with perforated silver discs making good contact with the effluent helium gas and thereby acting as a thermal exchange site between the bundle of electrical leads around the economizer and the considerable heat capacity of the cold effluent helium gas and minimizing vaporization of liquid helium from the reservoir. The calorimeter is surrounded by a cylindrical adiabatic shield. The top, bottom, and cylindrical sections of this shield are individually controlled by separate channels of automatic regulation which provide ac current to the respective shield heaters. Copper-Constantan thermocouples monitor the difference in temperature between calorimeter and shield and between shield and ring. Three separate channels of recording electronic circuitry provided with proportional rate and reset control actions were used for shield control above 50K. This instrumentation provided control of temperature to within about a millidegree over the temperature range and reduced the energy exchange between the calorimeter and surroundings so that it was negligible in comparison with other sources of error. Below 50K manual control of the adiabatic shield was employed. The manner of adiabatic operation employed has been described elsewhere.[1]

2. Calorimeter

The copper calorimeter (laboratory designation W-31) has a capacity of 50 cm^3 and was specially designed and constructed to make measurement on the rod-like, zone-refined cylinders of sample. It is in most essential details similar to one previously described[2] with the exception that no vanes are employed, that the thermometer well is located off center and projects through the bottom of the calorimeter for approximately a centimeter. The sample space has a diameter of 3.2 cm and an internal length of 6.3 cm. It is gold plated on all exterior and interior surfaces. The heat capacity of the empty calorimeter was determined in a separate series of measurements in which identical amounts of indium-tin (Cerroseal) solder for sealing the calorimeter and Apiezon-T grease for thermal contact with the

* - Submitted by Professor Edgar F. Westrum, Jr., University of Michigan, Ann Arbor, Michigan.

heater-thermometer assembly were used. At the lowest temperatures the heat capacity of the calorimeter-heater-thermometer assembly represented about 50% of the total. This increased to 74% at 20K, decreased again to 50% at 60K, then more gradually decreased to 30% at 140K, 20% at 200K, and 15% at 350K. Therefore, a favorable fraction of the total measured heat capacity was that of the sample over most of the range. The mass of the calorimetric sample was 165.246 gm (in vacuo). Buoyancy corrections were made on the basis of a density of ZrB_2 of 6.085 gm cm^{-3}. A pressure of 19.6 cm of helium at 300K was used to facilitate thermal conduction in the sample space.

Temperatures were determined with a capsule-type, strain-free, platinum resistance thermometer (laboratory designation A-5) contained with an entrant well in the calorimeter. A 150-ohm Constantan heater was bifilarly wound on a grooved cylindrical copper sleeve closely fitted to the resistance thermometer. Apiezon-T grease permitted the ready removal of this heater-thermometer from the calorimeter and hence the ready interchangeability of the calorimeters. Temperatures measured on this thermometer are considered to be in accord with the thermodynamic temperature scale within 0.03K from 10 to 90K and within 0.04K from 90 to 350K. Temperature increments may, of course, be determined with more precision than absolute temperatures and are probably correct to a few tenths of a millidegree after correction for quasi-adiabatic drift.

All measurements of resistance, potential, temperature, time, and mass are referred to calibrations made by the National Bureau of Standards.

3. Characterization and Purity of Sample

Because the procurement, purification, sintering, and zone refining of the zirconium diboride sample have already been described in considerable detail by George Feick in a previous report,[4] only certain salient features and analyses will be presented here in summary and in order to characterize the relatively high purity of the sample. The spectrographic analysis of the original sample provided by The Carborundum Company in ppm was: Al, Ca, Cr, Fe, Ni and Si, 100-500; Cu and Ti, 50-100; Mn, 500-1000. Spectrochemical analysis on samples obtained from various portions of the zone-refined rods indicated that the content of most of the metallic impurities were reduced by about an order of magnitude over that in the original sample, presumably by vaporization of impurities rather than by zone refining as such. These results were (in ppm): Ag, Cu, Ti, V, Cr, and Mn, 10; Al and Mg, 10-100; Hf and Fe, 10-1000; and Si, 100-1000. Two samples were reported to contain 48 and 65 ppm of oxygen. Triplicate analyses at various portions of the bar indicate that the carbon content approximates 215 ppm. With respect to the major constituents, averages of duplicate analyses on final ends of the bars (probably the least favorable region for purity and stoichiometry) were analyzed for zirconium and boron. The results are tabulated below:

	Sample A			Sample B		
	1	2	Ave.	1	2	Ave.
Zr	80.05	79.60	79.82	80.74	80.40	80.57
B	18.70	18.90	18.80	18.98	19.09	19.04
TOTAL			98.62			99.61
B/Zr ratio			1.96			1.99

These data suggest that the actual samples were very nearly (i.e., $\pm < 1\%$) stoichiometric and of purities in line with the analyses for minor constituents. The zone-refined rods were lightly etched in aqueous $HF-HNO_3$ to remove the film of oxide formed during zone refining, but were not further treated prior to measurement.

B. RESULTS

The experimental heat capacities are presented in chronological order at the mean temperatures of the determinations in Table I and graphically in Figure 9. These data are presented in terms of the defined thermochemical calorie equal to 4.1840 abs joule, an ice point of 273.15K and a gram formula weight of 112.864 for ZrB_2. These data have been corrected for curvature, i.e., for the difference between the measured $\Delta H/\Delta T$ and the limit as ΔT approaches 0. The approximate values of ΔT used in the heat capacity determinations can usually be estimated from the increments between adjacent mean temperatures shown in Table I. These heat capacity values are considered to have a probable error decreasing from less than 5% at 5K, to 1% at 10K and to less than 0.1% above 50K.

The heat capacities and thermodynamic functions at selected temperatures, as presented in Table II, are obtained from the heat capacity data by a least-squares-fitted curve through the experimental points (carefully compared with a large scale plot of the data) and the integration thereof. Both the fitting and the quadrature are performed by high-speed digital computers using programs previously described.[3] The thermodynamic functions are considered to have a probable error of less than 0.1% above 100K. An additional digit beyond those significant is given in Table II for internal consistency and to permit interpolation and differentiation. The entropies and Gibbs' energies have not been adjusted for nuclear spin and isotopic mixing contributions and are hence practical values for use in chemical thermodynamic calculations.

C. DISCUSSION

Tentative higher temperature enthalpy determinations on zirconium diboride have been reported by Professor John L. Margrave.[4,5] High accuracy is not to be anticipated in a derived function such as the heat capacity from enthalpy increment determinations near the temperature of the block into which the drop-calorimeter is equilibrated. However, the reported heat capacities at 300 and 400K of 13.16 and 15.29 cal gfw^{-1} K^{-1} from that study are higher by 14 and 8% than the direct determination of this quantity in the present research at 300K and the extrapolated one at 400K of 11.59 and 14.2 cal gfw^{-1} K^{-1}, respectively. It is, however, possible by the use of a Shomate plot[6] to reconcile the low temperature and high temperature heat capacity data except for determinations between 300 and 500K. The low temperature data can be faired into the high temperature data at about 600K. This would require an adjustment of about -240 cal gfw^{-1} in the enthalpy increment reported by Margrave at 600K and higher temperatures and a corresponding adjustment in the other functions. Because the high temperature values are tentative, are subject to change, and are furthermore privileged data, it was not considered proper to attempt a further correlation between the two sets of data.

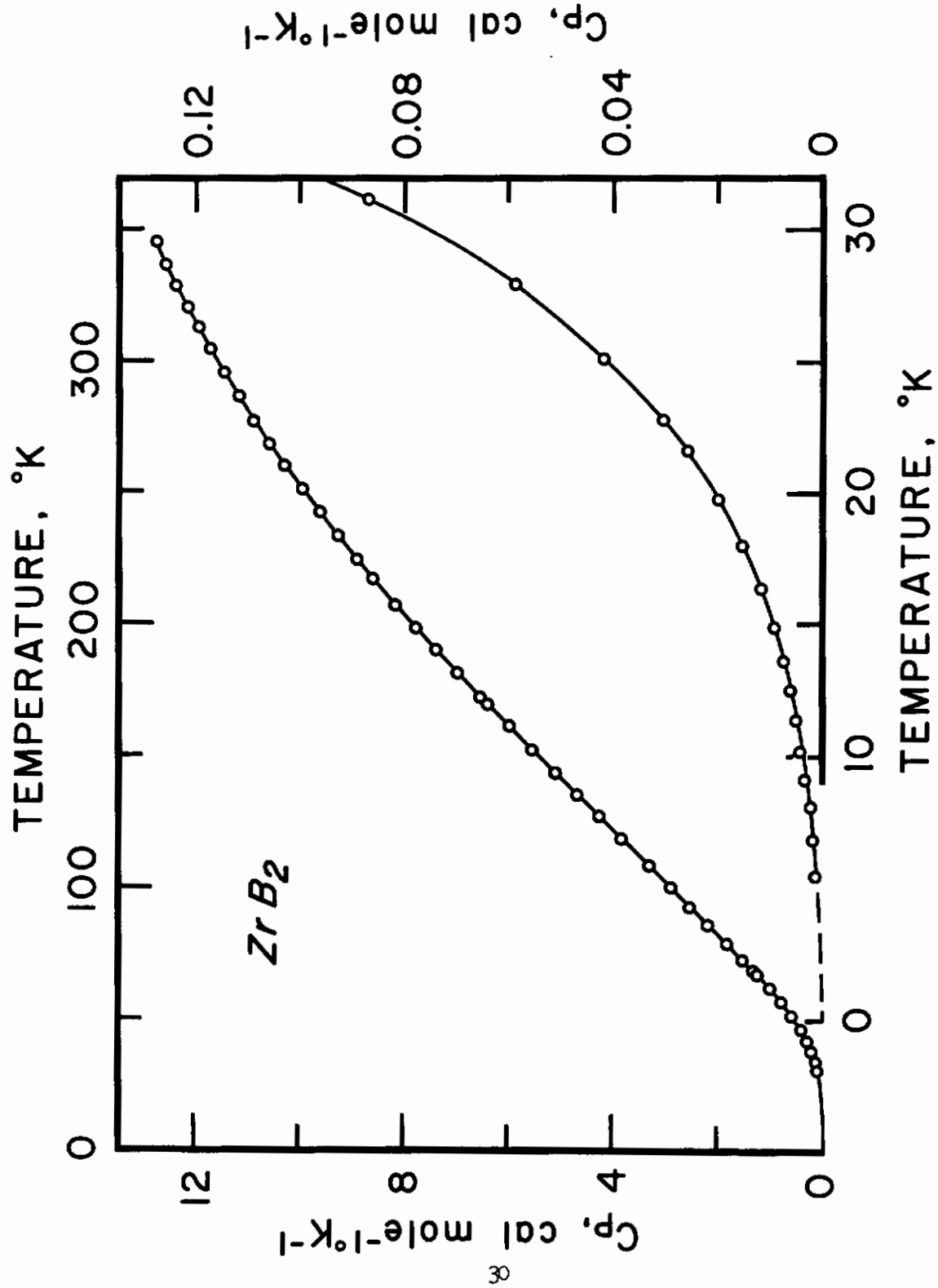

Figure 9. - Heat Capacity of Zirconium Diboride

TABLE I

HEAT CAPACITY OF ZIRCONIUM DIBORIDE

ZrB_2: gfw = 112.86 Units: cal gfw^{-1} K^{-1}

T, K	C_p	T, K	C_p	T, K	C_p
Series I		Series III		152.81	5.554
				161.47	5.992
67.62	1.2495	18.05	0.0154	169.96	6.411
73.24	1.518	19.76	0.0200	172.64	6.551
79.29	1.822	21.62	0.0259	181.64	6.975
86.15	2.176	22.80	0.0304	190.21	7.385
93.23	2.529	25.11	0.0417	198.74	7.781
100.79	2.905	27.90	0.0588	207.14	8.161
108.87	3.312	31.13	0.0868	217.19	8.601
		34.70	0.1309	224.60	8.920
Series II		38.37	0.1926	233.49	9.271
		42.29	0.2765	242.55	9.628
5.50	0.0015	46.80	0.3972	251.46	9.979
6.86	0.0019	51.88	0.5701	260.17	10.287
8.12	0.0023	57.41	0.7871	268.66	10.589
9.16	0.0035	62.44	1.0083	277.25	10.877
10.21	0.0044	68.91	1.3086	286.43	11.174
11.42	0.0051			295.78	11.460
12.55	0.0062	Series IV		304.56	11.729
13.67	0.0075			312.70	11.955
14.93	0.0093	119.42	3.850	320.44	12.165
16.41	0.0118	127.64	4.270	328.67	12.383
		135.78	4.686	336.97	12.576
		144.07	5.113	345.25	12.768

TABLE II

THERMODYNAMIC PROPERTIES OF ZIRCONIUM DIBORIDE

ZrB_2: gfw = 112.86 Units: cal., gfw, K

T	C_p	S°	H°	$(H°-H°_0)/T$	$-(F°-H°_0)/T$
5.00	0.001	0.0003	0.001	0.0003	0.0001
10.00	0.0037	0.0018	0.012	0.0012	0.0005
15.00	0.0094	0.0042	0.043	0.0029	0.0013
20.00	0.0206	0.0083	0.116	0.0058	0.0025
25.00	0.0408	0.0148	0.264	0.0106	0.0043
30.00	0.0762	0.0251	0.549	0.0183	0.0068
35.00	0.1354	0.0409	1.066	0.0304	0.0105
40.00	0.2250	0.0645	1.953	0.0488	0.0157
45.00	0.3456	0.0977	3.368	0.0749	0.0228
50.00	0.5026	0.1419	5.474	0.1095	0.0324
60.00	0.8986	0.2672	12.404	0.2067	0.0604
70.00	1.363	0.4400	23.67	0.3382	0.1018
80.00	1.858	0.6541	39.76	0.4970	0.1570
90.00	2.363	0.9021	60.87	0.6763	0.2258
100.00	2.870	1.1773	87.03	0.8703	0.3070
110.00	3.375	1.4745	118.26	1.0751	0.3994
120.00	3.881	1.790	154.54	1.288	0.5021
130.00	4.390	2.121	195.9	1.507	0.6137
140.00	4.900	2.465	242.3	1.731	0.7336
150.00	5.410	2.820	293.9	1.959	0.8608
160.00	5.917	3.185	350.5	2.191	0.9946
170.00	6.416	3.559	412.2	2.425	1.1134
180.00	6.904	3.940	478.8	2.560	1.2787
190.00	7.379	4.326	550.2	2.896	1.4298
200.00	7.840	4.716	626.3	3.132	1.584
210.00	8.286	5.109	707.0	3.367	1.743
220.00	8.717	5.505	792.9	3.600	1.905
230.00	9.134	5.902	881.3	3.832	2.070
240.00	9.534	6.299	974.6	4.061	2.238
250.00	9.919	6.696	1071.9	4.288	2.408
260.00	10.285	7.092	1172.9	4.511	2.581
270.00	10.635	7.487	1277.6	4.732	2.755
280.00	10.967	7.880	1385.6	4.949	2.931
290.00	11.285	8.270	1496.8	5.162	3.109
300.00	11.589	8.658	1611.2	5.371	3.287

TABLE II (Cont.)

ZrB_2: gfw = 112.86 Units: cal., gfw, K

T	C_p	S°	H°	$(H°-H°_0)/T$	$-(F°-H°_0)/T$
310.00	11.879	9.043	1728.6	5.576	3.467
320.00	12.155	9.424	1848.8	5.777	3.647
330.00	12.412	9.802	1971.6	5.975	3.828
340.00	12.648	10.176	2096.9	6.17	4.009
350.00	12.878	10.546	2224.6	6.36	4.190
273.15	10.74	7.611	1311	4.800	2.811
298.15	11.53	8.586	1590	5.332	3.254

Professor Margrave has further commented that there may be systematic errors in the lower temperature regions of their enthalpy determinations and that the data are not in good accord with measurements made on a different sample at Southern Research Institute.[5] The latter measurements are said to be between 10% and 20% higher than those of Professor Margrave over much of the common high temperature range. It is to be noted further that the measurements reported by Margrave were made on finely divided granular, less carefully characterized samples than those of the present research and that, in all probability, the ratio of heat capacity of sample to that of sample plus capsule was not as favorable. In any event, in view of the high quality of the present samples and the nature of the measurements involved, data from the present research are recommended as the more reliable over the range of overlap.

Acknowledgement: The assistance of Ray Radebaugh and Merritt Hougen in the operation of the calorimetric cryostat is gratefully acknowledged. The major contributions to this study is of course that of Mr. George Feick without whose ingenuity and persistent endeavors this research would have been without a calorimetric sample.

V. HIGH TEMPERATURE HEAT CONTENT STUDIES*

A. EXPERIMENTAL RESULTS FOR ZrB_2, HfB_2 AND ZrC

The high temperature heat contents of HfB_2, ZrB_2 and ZrC have been determined using a drop calorimeter which was designed by Dr. Robert Grimley and has been used for a number of other high temperature studies.[7] In this calorimeter a sample contained in a metal protective capsule is heated in a platinum resistance furnace to the desired temperature and then dropped into a copper block of known heat capacity. Gold capsules were used as containers and thus the upper limit of study was about 1200K. No reactions were observed between the samples and the capsules.

The samples were provided by The Carborundum Company through the courtesy of Dr. Peter Schaffer. X-ray analysis showed only one phase present. The high temperature heat contents were calculated with a CDC-1704 program directly from the experimental data.

In Tables I, II and III are presented the experimental data and in Tables IV, V and VI are smoothed thermodynamic functions calculated from the data along with an equation derived by the least squares technique. This equation is only guaranteed to fit reliably within the limits indicated and extrapolation to lower or higher temperatures is questionable.

B. DISCUSSION

A series of somewhat parallel measurements on refractory borides and carbides has been reported by the Southern Research Institute, WADD TR-60-924. A comparison of our results with data from Southern Research Institute shows a large discrepancy, far beyond either acknowledged experimental error. We are presently reviewing our calibration and calculational procedures to seek out any sources of error. Intercomparisons with other laboratories on a variety of samples are in progress.

Very recent correspondence with Professor E. F. Westrum concerning his ZrB_2 data at low temperatures (cf. Section IV, this report) shows that there is some deviation of the 400-600K points from the smooth extrapolation of Westrum's data to the highest temperature points. The cause of this deviation is being examined. It is also worth noting that the Southern Research Institute data deviate very drastically from Westrum's data and do not extrapolate at all.

As part of an effort to derive a better equation for fitting and extending high temperature data, a program has been developed in collaboration with Dr. R. L. Altman to fit Debye-Einstein functions to the experimental data. This equation has a better form for extrapolation and can give excellent fits of the data. When a good fit is possible, one can estimate S_{298} and other important thermodynamic properties with high reliability. From a curve fitting of the high temperature data we estimate S_{298} for ZrC to be 8.7 ± 0.5 entropy units.

* Prepared from reports submitted by Professor John L. Margrave, University of Wisconsin, Madison, Wisconsin.

Finally, to extend the measurements to higher temperatures we have procurred a high frequency induction heater to replace the platinum-wound furnace and permit operation to 2000C. Modification of the furnace unit is in progress.

TABLE III

EXPERIMENTAL RESULTS FOR ZrB_2

Temperature, K		Enthalpy, Cal/mole	
Sample (T_1)	Calorimeter (T_2)	$H_{T_1} - H_{T_2}$	$H_{T_1} - H_{298.16}$
429.30	298.99	1,890	1,899
521.10	299.07	3,422	3,432
634.30	299.13	5,271	5,281
917.60	299.53	10,649	10,664
1,048.50	299.56	13,020	13,035
1,171.60	299.82	15,636	15,654

TABLE IV

EXPERIMENTAL HEAT CONTENTS OF HfB_2

T, K	$H_T - H_{298}$ (exptl)
486.3	2789.1
677.4	5916.4
745.7	7156.0
773.8	7723.8
816.7	8327.5
873.4	9350.3
890.8	9914.7
950.0	10977.2
994.3	11737.3
1023.7	12443.6
1082.8	13620.5
1130.3	14540.0
1149.9	14885.8

TABLE V

EXPERIMENTAL RESULTS FOR ZrC

Temperature, K		Enthalpy, Cal/mole	
Sample (T_1)	Calorimeter (T_2)	$H_{T_1} - H_{T_2}$	$H_{T_1} - H_{298.16}$
470.80	298.81	1,833	1,839
603.40	299.00	3,337	3,345
735.40	298.98	4,881	4,889
863.00	299.00	6,446	6,454
973.00	299.16	7,875	7,884
1,174.40	299.16	10,381	10,390

TABLE VI

HIGH TEMPERATURE THERMODYNAMIC FUNCTIONS FOR ZrB_2

T (K)	$H_T - H_{298.16}$ (cal $mole^{-1}$)	Cp (cal $mole^{-1} deg^{-1}$)	$S_T - S_{298.16}$ (cal $mole^{-1} deg^{-1}$)
300	24	13.16	0.08
400	1,459	15.29	4.19
500	3,052	16.50	7.74
600	4,747	17.35	10.83
700	6,517	18.03	13.56
800	8,350	18.62	16.01
900	10,239	19.15	18.23
1000	12,180	19.66	20.27
1100	14,169	20.14	22.17
1200	16,307	20.60	23.94

$$H_T - H_{298.16} = 15.81\ T + 2.10 \times 10^{-3} T^2 + 3.52 \times 10^{5} T^{-1} - 6,081$$

$(\pm\ 1.2\%,\ 429 - 1171K)$

$$Cp = 15.81\ T + 4.20 \times 10^{-3}\ T - 3.52 \times 10^{5} T^{-2}$$

TABLE VII

HIGH TEMPERATURE THERMODYNAMIC FUNCTIONS FOR HfB_2

T (K)	$S^o_T - S^o_{298}$ (cal/mole/deg)	$H^o_T - H^o_{298}$ (cal/mole)
500	7.73	3035
600	10.69	4656
700	13.30	6356
800	15.68	8134
900	17.86	9990
1000	19.90	11925
1100	21.82	13938
1200	23.64	16030

$$H_T - H_{298} = 11.89\ T + 3.923 \times 10^{-3} T^2$$

$$-3,895 \text{ cal/mole}$$

$$Cp = 11.89 + 7.846 \times 10^{-3}\ T \text{ cal/mole-deg}$$

TABLE VIII

HIGH TEMPERATURE THERMODYNAMIC FUNCTIONS FOR ZrC

Temp (K)	$H_T - H_{298.16}$ (cal $mole^{-1}$)	Cp (cal $mole^{-1}deg^{-1}$)	$S_T - S_{298.16}$ (cal $mole^{-1}deg^{-1}$)
300	18	9.75	0.06
400	1,052	10.80	3.03
500	2,162	11.36	5.50
600	3,317	11.73	7.61
700	4,504	12.01	9.44
800	5,717	12.24	11.06
900	6,951	12.44	12.51
1000	8,205	12.63	13.83
1100	9,476	12.80	15.04
1200	10,764	12.97	16.16

$$H_T - H_{298.16} = 11.40\ T + 0.71 \times 10^{-3} T^2 + 18.67 \times 10^{4} T^{-1} - 4,087$$

($\pm$ 0.7%, 471 - 1,174°K)

$$Cp = 11.40 + 1.42 \times 10^{-3} T - 18.67 \times 10^{4} T^{-2}$$

VI. MASS SPECTROMETRY*

A. BACKGROUND

Knowledge of gaseous species formed during the vaporization or decomposition of refractories and during the reaction of refractories with various atmospheres is an essential requirement preliminary to a quantitative analysis of their behavior at high temperatures. The outstanding tool for such studies is the mass spectrometer. We shall report here the results of a study of the vaporization of zirconium diboride, and shall discuss in this connection some general aspects of the vaporization of binary refractory compounds. Preliminary work on gas-solid reactions will also be discussed.

B. THE VAPORIZATION OF ZIRCONIUM DIBORIDE

The vaporization of samples of zirconium diboride of composition $ZrB_{2.05}$ and $ZrB_{1.96}$ was examined mass spectrometrically. Zirconium and boron atoms were found to be the only vapor species present. The equilibrium vapor pressure above condensed zirconium boride may, therefore, be calculated from the heat of formation[8] and high temperature thermal functions of $ZrB_2(s)$ (cf. Section V), and by the heats of sublimation[9] and high temperature thermal functions[9] of gaseous boron and zirconium.

1. The Mass Spectrometer

The mass spectrometer used in these experiments is a 12-inch radius, 60°-sector direction-focusing instrument designed by Professor Mark G. Inghram, of the University of Chicago, and built by Nuclide Analysis Associates of State College, Pennsylvania. In the experiments to be described, the sample was heated in a Knudsen cell with a 1 mm diameter orifice. The molecular beam thus generated was ionized by 60-volt electrons and the positive ions formed accelerated through a 4000-volt potential. After mass analysis, ions were detected by means of an electron multiplier whose output was measured by a vibrating-reed electrometer and displayed on a recording potentiometer.

In an initial test of the performance of the mass spectrometer, a sample of hafnium carbide was heated in a tungsten Knudsen cell to temperatures up to 2450K. No species resulting from the evaporation of hafnium carbide were observed, although at least evaporation of carbon was expected. At the end of the experiment, however, it was found that considerable deformation of the crucible support system had occurred, so that the crucible orifice was no longer properly aligned with respect to the entrance slit of the ionization chamber. To improve the structural stability of the system, the thickness of the Inconel plate holding the crucible support rods (cf. Figure 10, which also shows the arrangement for gas-solid reactions) and the diameter of the Vycor tubes serving to align the support plate with the bottom flange both were doubled. That these modifications were successful was demonstrated in the zirconium diboride experiment, in which data were obtained at crucible temperatures up to 2650K.

* - Submitted by Dr. Alfred Buchler, Arthur D. Little, Inc., Cambridge, Mass.

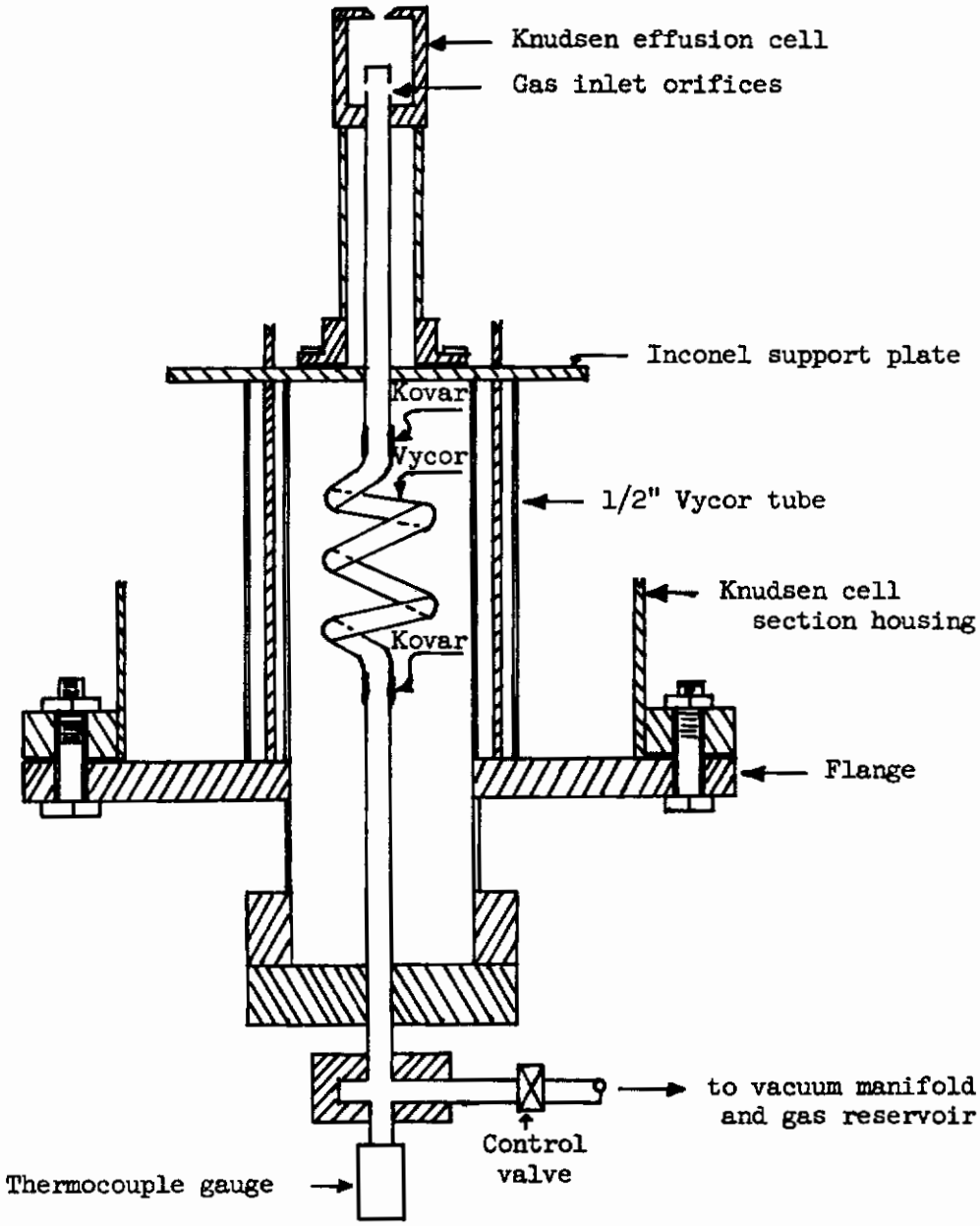

Figure 10. - Mass Spectrometer Knudsen Cell Section as Modified to Permit High Temperature Flow Experiments

2. Zirconium Diboride Experiments

Samples of zirconium diboride of composition $ZrB_{2.05}$ and $ZrB_{1.96}$ were provided by G. E. Feick (see Section III for preparation details). The first of these samples was heated in a molybdenum crucible. Boron and zirconium atoms were observed in the vapor. Measurement of high temperatures was made difficult by the blackening of the pyrometer viewing window by evaporated molybdenum. However, it was possible to estimate a value of $I_{B^+}/I_{Zr^+} = 4$ for the ratio of boron and zirconium ion currents near 2300K.

For the $ZrB_{1.96}$ sample, a tungsten crucible was used, and the ion intensities of Zr^+ and B^+ measured over a temperature range from 2300 to 2650K. The results are plotted on Figure 11, where use has been made of the relation

$$p = kIT \qquad (1)$$

where p is the partial pressure, I the ion current, T the absolute temperature, and k a proportionality constant to be discussed below. The values given in Figure 11 correspond to the isotope ions $(Zr^{90})^+$ and $(B^{11})^+$. Correcting for isotopic abundances, one obtains for the total ion current ratio a value of $I_{B^+}/I_{Zr^+} = 2$. In this experiment, a search was made for ions corresponding to compounds of formulas ZrB, ZrB_2, and Zr_2B_2. No evidence for the existence of any of these compounds was found. It was concluded, therefore, that ZrB_2 vaporizes by decomposition to the elements.

3. Discussion

For the further interpretation of these results, a number of questions have to be examined. These include:

a. The relation of the observed ion intensity ratio to the composition of the vapor in the crucible.

b. The composition of the condensed phase and its relation to the observed vapor pressure.

c. The relation of the observed temperature dependence of partial pressures to the thermal properties of the condensed phase.

a. Ion Intensity and Vapor Composition

To obtain the composition of the vapor in the Knudsen cell from the observed ion ratio, the latter has to be corrected for the relative ionization cross sections of the corresponding neutral species and for the relative detection efficiency of the electron multiplier for the various ions. We can neglect the latter correction, since experiments which we have carried out on the relative efficiency of detection of lithium and silver ions show that the detection efficiency of our multiplier is reasonably independent of mass for monatomic ions. For the relative ionization cross sections, the calculations of Otvos and Stevenson[10] are generally used. From their values an ionization cross-section ratio of $\sigma_{Zr}/\sigma_{B} = 12$ is obtained, which, when applied to the observed ion ratio, yields a ratio of partial pressures of

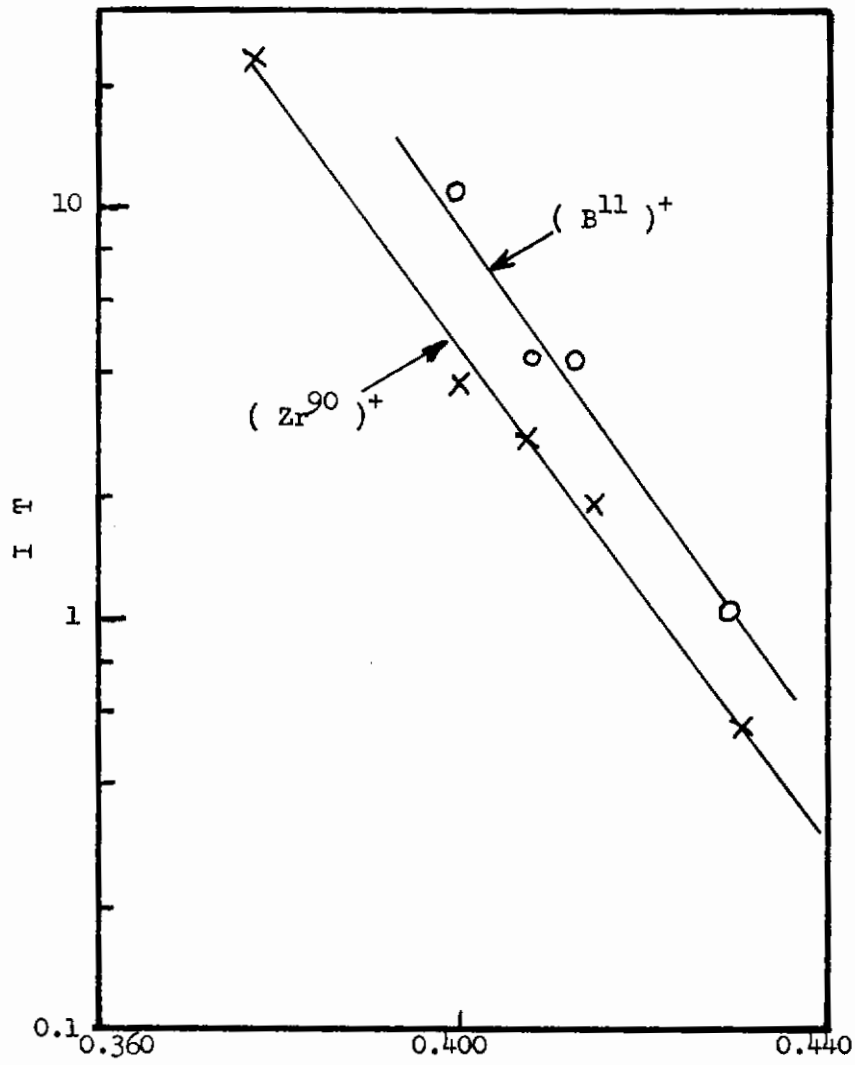

Figure 11. - Experimental Data from $ZrB_{1.96}$ Evaporation

$P_B/P_{Zr} = 24$ for the vapor above $ZrB_{1.96}$. This ratio appears to be too high, though, for reasons to be discussed below, it cannot be ruled out. It is clear that one of the most urgent problems in the mass-spectrometric analysis of vapors of this type is the experimental determination of relative ionization cross sections.

b. Effect of the Nature of the Condensed Phase

In compounds of the zirconium boride type, a Knudsen cell experiment presents an interaction of thermodynamic and kinetic factors whose analysis is important both from the point of view of the interpretation of the experiment and from that of the behavior of the compound in possible practical applications. In the following discussions, we make three assumptions throughout.

1. The vapor in the Knudsen cell is at all times in thermodynamic equilibrium with the condensed phase.
2. The relative rates at which boron and zirconium effuse from the crucible is given by the gas-kinetic relationship

$$\frac{Z_B}{Z_{Zr}} = \frac{P_B}{P_{Zr}} \left(\frac{M_{Zr}}{M_B}\right)^{1/2} = 2.90 \frac{P_B}{P_{Zr}} \qquad (2)$$

   where Z refers to the rate of effusion in moles per unit time and M to the atomic weight.
3. The condensed phase is homogeneous, i.e., we neglect the possible effect of diffusion in the solid on the evaporation process.

With these assumptions, we can now discuss two possible situations as to the nature of the condensed phase: first, that a compound of the formula ZrB_x, where $x \sim 2$, vaporizes congruently, and, secondly, that a range of homogeneity exists near the composition ZrB_2.

Congruent evaporation of ZrB_x implies that the composition of the solid phase remains unchanged by evaporation under all conditions of temperature and pressure. In this case, a sample of ZrB_x in equilibrium with its own vapor in a closed cell will constitute a one-component system from the point of view of the phase rule, since a single composition variable serves to describe both solid and gas phase. With two phases present, we obtain for the number of degrees of freedom $F = C - P + 2 = 1$. Thus, selection of, say, the temperature fixes the pressure and the system has a unique vapor pressure. The partial pressures corresponding to this case, with $x = 2$, are shown by the full lines in Figure 12.

The situation changes if a mechanism exists for varying the composition of the gas phase. In the case of the Knudsen experiment, such a mechanism is provided by the preferential effusion of boron. We now deal with a two-component system and,

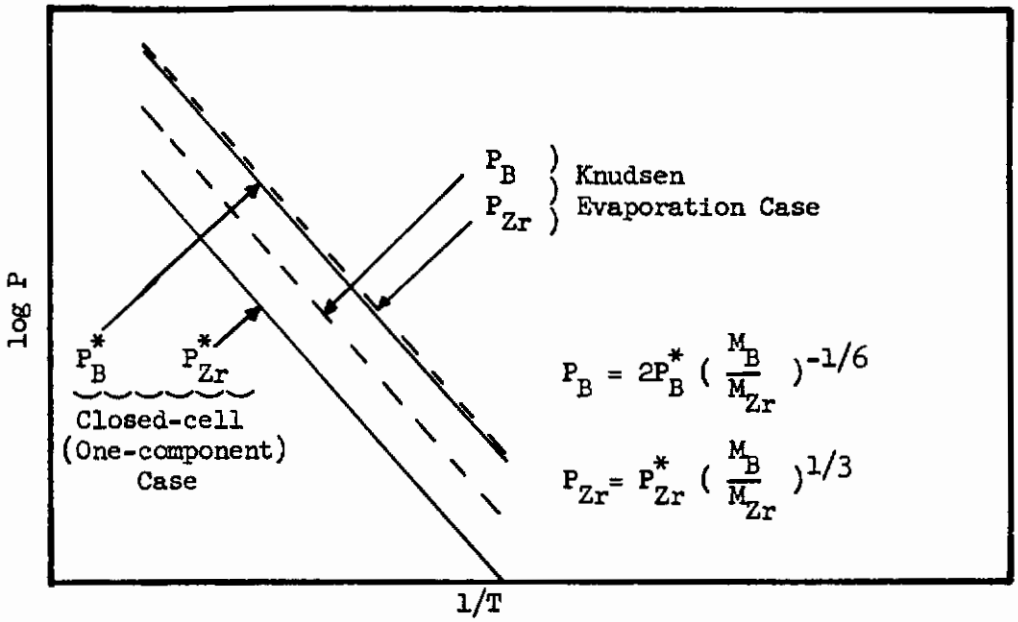

Figure 12. - Vapor Pressure Diagram
for Congruently Evaporating ZrB_2 (Hypothetical)

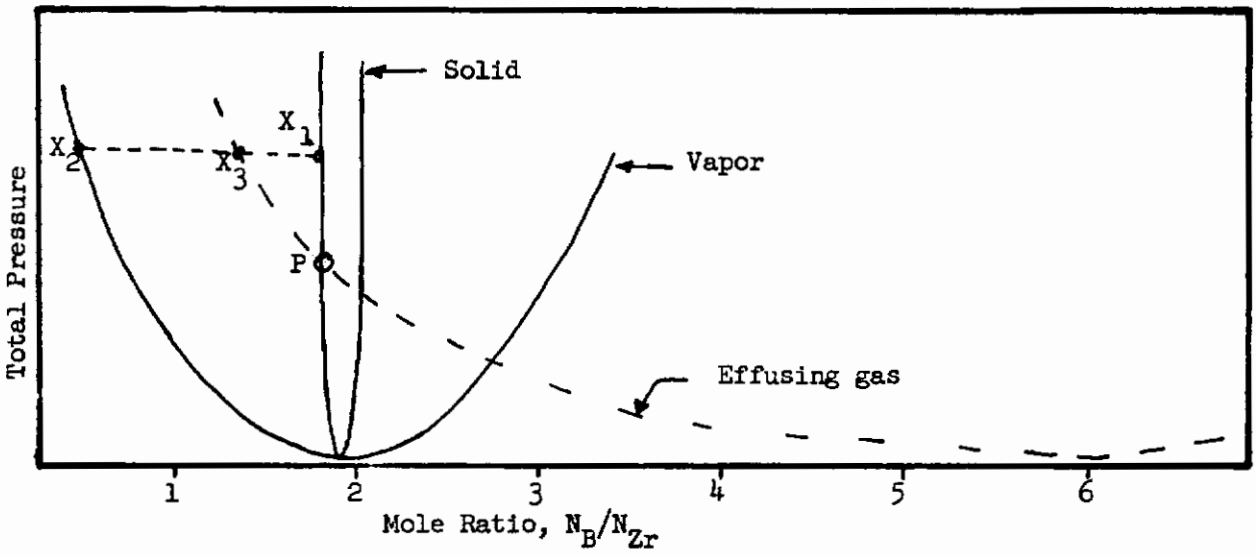

Figure 13. - Constant Temperature Phase Diagram (Hypothetical)

therefore, with two phases present, with two degrees of freedom. The possible variables are the composition of the gas phase, the pressure, and the temperature, the relation between them being given by the equilibrium constant

$$K(T) = P_{Zr} P_B^{\,x} \qquad (3)$$

In the Knudsen evaporation case, the composition of the gas phase under steady-state conditions is determined by the requirement that the composition of the effusing gas is equal to that of the solid. From Equation 2 we then have

$$\frac{P_B}{P_{Zr}} = \frac{x}{2.90} \simeq \frac{2}{3} \qquad (4)$$

This ratio is independent of temperature, and the resulting partial-pressure curves, again for x = 2, are given by the dotted lines of Figure 12.

The existence of a homogeneity range in the vicinity of the composition ZrB_2 requires treatment of the condensed phase as a solid solution. There are four variables: the compositions of the solid and gas phases, the temperature and the pressure. Two of these have to be fixed to define the state of the system. A hypothetical phase diagram for a given temperature is shown in Figure 13, where total vapor pressure is plotted against composition of solid and gas, expressed in terms of the mole ratio n_B/n_{Zr}. Here we have assumed the two curves to be tangent at the composition $ZrB_{1.9}$, which then corresponds to the equivalent of a constant-boiling composition in constant-temperature equilibrium distillation. On the boron-rich side of the diagram, the equilibrium vapor composition is always richer in boron than the solid composition, whereas the opposite holds on the zirconium-rich side of the diagram. It should be noted that in the present case an equilibrium constant cannot be defined, since the free energy of formation of the solid phase will change over the range of homogeneity: for a given temperature, the partial pressures of boron and zirconium have unique values for each composition of the solid phase, and a change in the partial pressure in one of the component gases will produce a change in the composition of the solid.

In the mass-spectrometric Knudsen-cell experiment, we fix the temperature and the initial composition (say, at X_1). The composition of the vapor in the cell is then given by X_2. The composition of the gas effusing from the cell is given by the point X_3 on the dotted curve, which is related to the gas composition curve through Equation 2. It is clear that prolonged evaporation will lead to a decrease in the boron concentration in the solid. A steady state will be reached at the composition corresponding to the point P where the composition of the solid is equal to that of the effusing vapor. This point, therefore, represents a second type of "constant-boiling" composition. It is worth pointing out that if the evaporation coefficients of zirconium gas and boron gas from the solid phase are equal, the point P also gives the "constant-boiling" composition obtained in the free evaporation of zirconium diboride. For other values of the evaporation coefficients, this "free-evaporation constant-boiling composition", which may be important from a practical point of view, will be determined by the relative rates of evaporation of zirconium and boron, rather than by any feature of the phase diagram.

c. The Temperature Coefficient of Partial Pressure

The slopes of the log p vs. 1/T plots of Zr(g) and B(g) give the partial heats of sublimation, $\Delta \bar{H}_s(B)$ and $\Delta \bar{H}_s(Zr)$, as long as the composition of the solid phase remains constant. The last condition is always fulfilled in the gas of congruent evaporation. If there is a range of homogeneity, the composition of the solid phase effectively remain constant if a large enough sample is used and if the temperature range is traversed during a short enough time. In both cases, therefore, we can write for the heat of formation of $ZrB_x(c)$ from the gaseous atoms

$$- \Delta H_f(ZrB_x,C) = \Delta \bar{H}_s(Zr) + x \Delta \bar{H}_s(B)$$

While, however, the two partial heats, and hence the two slopes, will be equal in the congruent-evaporation case, this will not be so in the case of a range of homogeneity.

4. Conclusions

Our experiments show that (1) zirconium diboride vaporizes by decomposition to the elements and that (2) it possesses a homogeneity range in the vicinity of $ZrB_{1.96}$. The latter conclusion is based on the observation that the boron/zirconium ratio in the vapor is at least 2, and probably considerably higher, whereas the ratio for a congruently evaporating solid would be of the order of 2/3. Our finding is in accord with the phase diagram given by Glaser and Post.[11]

Largely because of difficulties of temperature control, the number of points obtained in the $ZrB_{1.96}$ experiment was quite limited. Nevertheless, slopes were calculated in order to check whether the observed temperature dependence of partial pressure was at least consistent with what is known of the thermodynamics of the system. We obtain

$$\Delta \bar{H}_s(Zr) = 135 \pm 10 \text{ kcal/mole}$$

$$\Delta \bar{H}_s(B) = 144 \pm 18 \text{ kcal/mole}$$

and for the reaction

$$Zr(g) + 1.96\ B(g) \longrightarrow ZrB_{1.96}(C), \quad 2500K$$

$$\Delta H = - 417 \pm 45 \text{ kcal/mole}$$

The result is of the same magnitude as the second-law heats obtained by Leitnaker,[12] who, however, analyzed his data in a manner which implies congruent evaporation. From the data given in JANAF Interim Thermochemical Tables, we obtain a value of 384 kcal for the vaporization of Zr(l) + 1.96 B(l) at 2500K, so that our data would give -31 kcal/mole for the heat of formation of $ZrB_{1.96}$ from the elements at 2500K, a value which is almost certainly considerably too low. A value of -76 kcal/mole quoted by Leitnaker from the unpublished work of Huber, Head and Holly is, however,

just within the range of our experimental error. At the present stage, it would seem most important to obtain calorimetric heats of formation of zirconium diboride over the range of homogeneity, since, given that vaporization occurs only to the elements, the reverse of the present calculation can then be used to predict vapor pressures.

C. FLOW EXPERIMENTS

1. Gas Handling System

In the present system, gas is introduced from an external gas handling system into the Knudsen cell section of the mass spectrometer (see Figure 10). The pressure at the inlet to the mass spectrometer is read on a thermocouple gauge. Reaction takes place in an effusion cell into which the gas flows through a number of small orifices. When electron bombardment is used to heat the cell, the latter may be at potentials of up to 1000 volts above ground; hence, part of the gas line inside the mass spectrometer consists of a Vycor helix which insulates the flow cell from the mass spectrometer housing.

To test the flow system from the point of view of the pressures attainable, argon gas was permitted to stream into a dummy flow cell consisting of a tube which could be provided with a single orifice of varying size. The pressures in the Knudsen cell, ion source and analyzer section of the mass spectrometer were measured as a function of the pressure at the gas inlet. The results are graphed in Figures 14 and 15. It must be remembered that the limiting experimental pressure is set by the requirement that the pressure in the ion source region should not exceed 10^{-5} mm. This requirement produced a limiting inlet pressure of 0.015 mm with an orifice of 1 mm diameter. Reduction of the orifice area by a factor of 10 increased the limiting pressure to 0.1 mm. Further increases in the limiting pressure will require an increase in the pumping speed available.

During the experiments just described, the mass peak corresponding to argon ion was continuously monitored on the mass spectrometer. It was found that the intensity of the mass spectrometric signal observed was directly proportional to the gas inlet pressure and followed changes of the inlet pressure very rapidly, indicating a very low hold-up in the flow system. These results are of considerable significance for the experiments we have planned. The standard test for discriminating between background ions and ions corresponding to material effusing from the Knudsen cell consists of placing a shutter in the molecular beam. This test does not work in the case of permanent gases, but the proportionality of inlet pressure and signal observed provides a way around this difficulty.

2. Preliminary High Temperature Flow Experiments

In a first experiment on the zirconia-water vapor system, zirconium oxide powder was heated in a molybdenum flow cell to a temperature up to 2230K. Water was introduced at an inlet pressure of 0.1 mm. It may be noted that a significant amount of dissociation of water will take place at the crucible temperature. Against expectations, no reaction products were observed. A possible reason for

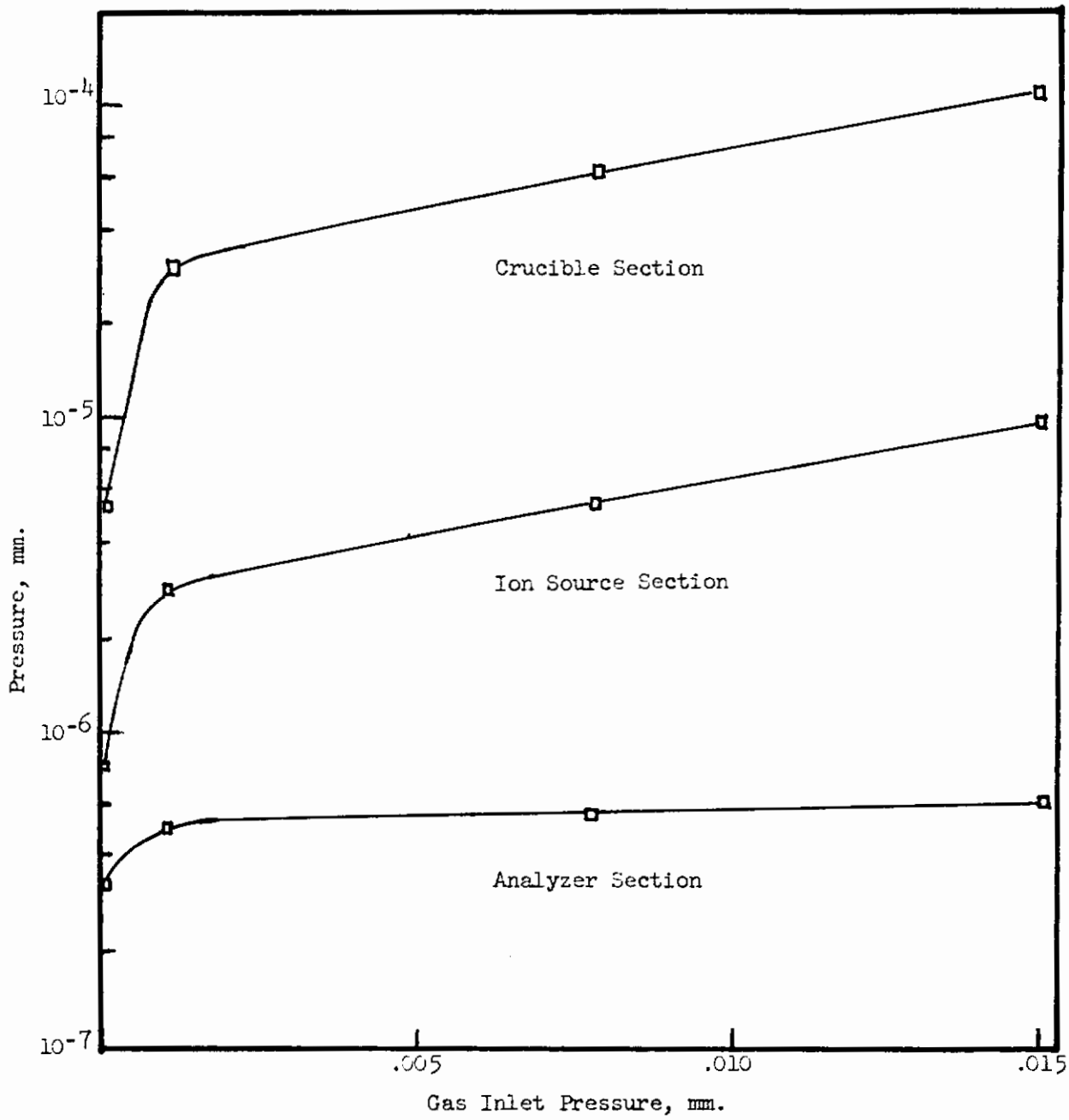

Figure 14. - Pressure Data for Flow System Test with 1 mm Diameter Orifice

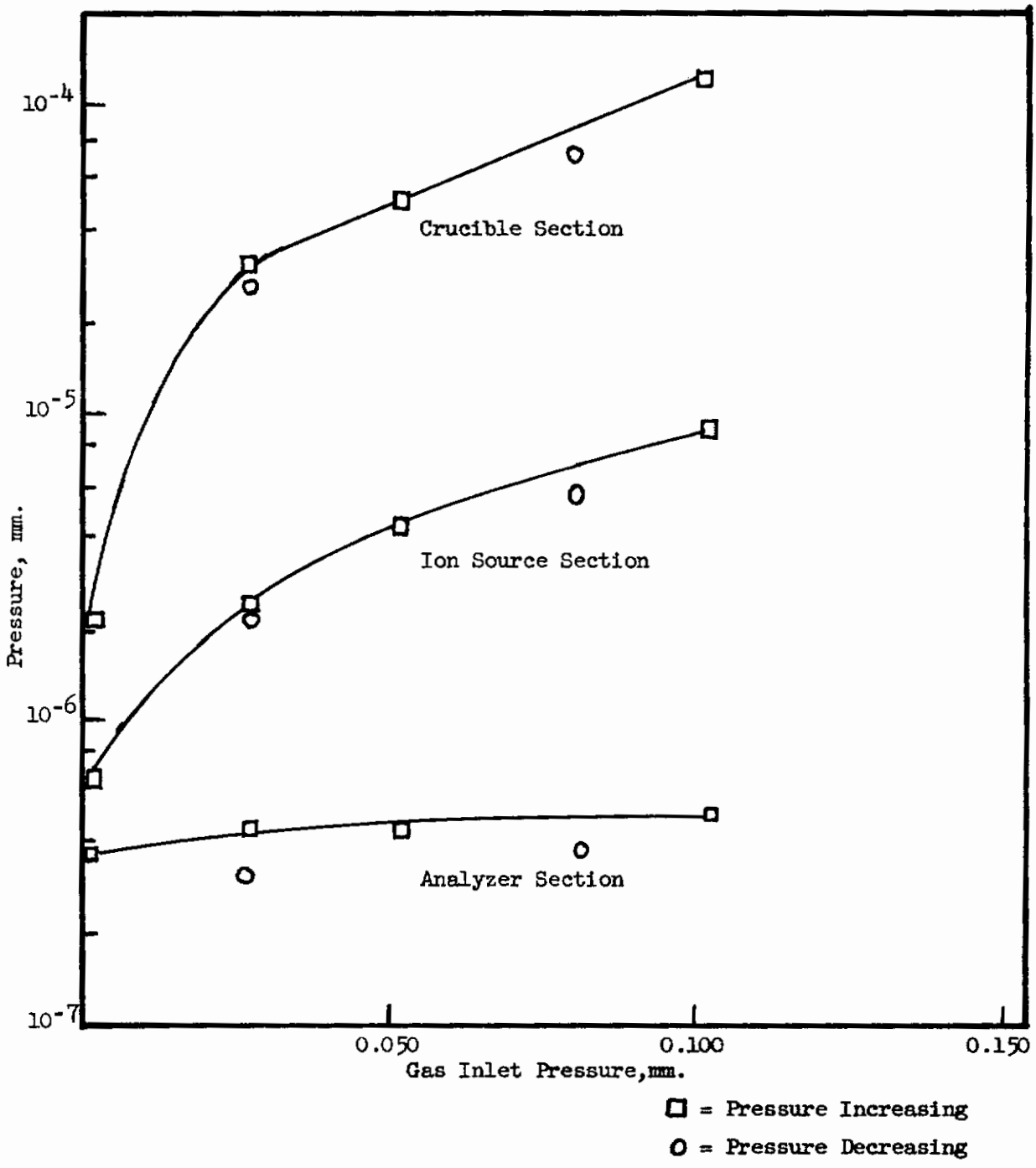

Figure 15. - Pressure Data for Flow System Test with 0.32 mm Diameter Orifice

this situation is a slow rate of reaction between the water vapor and the oxide. This hypothesis is borne out by experiments in which boron trifluoride gas was passed over boron oxide. For this sytem, the equilibrium thermodynamic properties have been studied independently by means of solid-solid reactions. In the gas-solid experiments, both the ratio of boron oxyfluoride trimer and monomer and the absolute amount of these products were found to be considerably different from the quantities expected under equilibrium conditions.

Some encouraging conclusions, however, followed from the zirconia-water vapor experiments. Attainment of high temperatures was not interfered with by the introduction of the gas flow system, even though the radiation shielding of the crucible had to be significantly decreased. While the problem of attaining and maintaining high temperatures has thus been solved, the problem of reaction kinetics still remains. In the experiments currently planned, therefore, we will introduce two modifications. First, a tantalum flow cell with a zirconium oxide liner will be used in order to produce the largest possible area of contact between zirconium oxide and water vapor. Second, the pumping speed available will be increased to permit vapor pressure of at least 1 mm in the effusion cell. These modifications will reduce considerably the effect of chemical kinetics on the attainment of equilibrium in the flow cell and should lead to a definite decision as to the existence of a gaseous zirconium hydroxide.

VII. SPECTROSCOPY OF HIGH TEMPERATURE SPECIES BY MATRIX ISOLATION*

A. INTRODUCTION

The study of the infrared absorption spectra of molecules characteristic of high temperature systems is of prime importance since the knowledge of the vibrational states allows the calculation of thermodynamic functions by the methods of statistical mechanics. In addition, the structure of these molecules as investigated by these spectra is of interest to theoretical chemistry. The main difficulties encountered in such investigations in the vapor phase are due to the experimental problems and due to the complexity of the vibration-rotation spectra at these high temperatures.

The present project has as its aim the investigation of the feasibility of an alternate technique. The solid is vaporized in a small effusion cell and the vapor is allowed to impinge on a cold salt window kept at liquid helium temperature while at the same time an inert gas is deposited there. In this way, the isolated molecules which are the vaporization products of the solid are trapped and kept isolated one from the other by the "matrix cage" surrounding them. The method is adapted from the so-called "matrix isolation technique"[13] and has been applied to lithium fluoride by Linevsky.[14]

To date, the matrix spectra of lithium fluoride have been obtained in this work. The results reported previously have been confirmed and new absorptions have been observed whose assignment is discussed. The investigation is continuing and is being extended beyond the sodium chloride region. It is important to first investigate a series of substances whose vapor spectra are known so that the results obtained can be compared and the matrix perturbation can be investigated. For this reason the alkali halides are an obvious choice since they have been investigated by Klemperer and coworkers[15] and by Vidale.[16] Klemperer and Norris[17] have very recently also observed absorptions which they assign to the dimers of the lithium halides. These dimers have been known for some time to exist in appreciable concentration in the vapor.[18]

As a part of the plan to investigate matrix perturbations of polar molecules the infrared spectrum of hydrogen chloride in rare gas matrices has been studied.

Preparations have been made for the study of very high boiling substances by the present technique. An electron bombardment oven has been built for this purpose which is suitable for use with the low temperature cryostat.

B. EXPERIMENTAL

A helium cryostat is fitted with a sodium chloride window which is cooled by the liquid helium. An inlet tube admits a gas which impinges on the cold window and is deposited as a solid film. This gas stream is directed at the cold window at an angle of 45° to it. A small evaporation oven is built into the cryostat such that a molecular beam emerges from it and the molecules in it impinge on the cold window at the same time as the gas stream but from another direction.

* - Submitted by Professor Otto Schnepp, Technion - Israel Institute of Technology, Haifa, Israel.

The vaporization oven, as used in the experiments described in this report, consisted of a tantalum sheet effusion cell heated by radiation from a resistance heated tantalum strip. The temperature in the effusion cell was controlled by means of a chromel-alumel thermocouple. By this technique dilute solid solutions of cesium chloride, lithium chloride, or lithium fluoride in solid argon, krypton, and nitrogen were prepared and their spectra investigated.

Preliminary experiments were carried out to investigate the rate at which the salt vapor impinged on the window by observing the interference colors due to the salt film on the window. It was found that the results agreed very closely with calculations based on the assumption that effusive conditions prevailed in the case of cesium chloride and lithium chloride. For the case of lithium fluoride, on the other hand, the observed rate was found to be one third to one tenth that predicted but the results were very reproducible from experiment to experiment.

During a typical matrix experiment the effusion cell was kept at a temperature corresponding to a vapor pressure of 10 microns. The infrared spectra of lithium fluoride was clearly observable after half an hour of deposition.

In another series of experiments hydrogen chloride was mixed with argon, krypton, and xenon and in ratios of 1:100, 1:300, and 1:1000 and this gas mixture was deposited on the cold window by means of the gas admission tube. In these experiments the vaporization oven was not used.

The ultraviolet spectra were studied on a medium quartz spectrograph using a high-pressure xenon arc as source. The infrared spectra were studied on a Perkin-Elmer Model 21 double beam spectrophotometer using sodium chloride and calcium fluoride optics.

C. RESULTS

No absorption spectra in the ultraviolet were observed for cesium chloride or lithium chloride in matrices.

Infrared spectra were observed for lithium fluoride in argon, krypton, and nitrogen at 4.2K. In argon the absorption consists of two peaks of frequencies 836 and 841 cm^{-1}, the lower energy peak being the more intense one. In krypton the absorption is a single peak at 831 cm^{-1} and in nitrogen it was also a single peak at 776 cm^{-1}. The band width was about 5 cm^{-1} in each case. These observations are in complete accordance with those reported by Linevsky.[14] In addition to these bands, lithium fluoride in argon has an absorption at 721 cm^{-1} and in krypton an absorption at 717 cm^{-1}. In nitrogen no additional absorption band was observed in the sodium chloride region.

The infrared spectrum of hydrogen chloride in rare gas matrices at 4.2K at the lowest concentration used here consists of a single line whose frequency is 2891 cm^{-1} in argon, 2875 cm^{-1} in krypton, and 2857 cm^{-1} in xenon. The 0-1 transition in the gas phase is at 2906 cm^{-1}. At higher concentrations and at 20K, additional features were observed. At 20K in argon and krypton the main lines

were accompanied by satellites 20 cm^{-1} to higher energy and 40 cm^{-1} to lower energy. These satellites were not completely resolved from the central line. To lower energy three additional bands were observed displaced by 70 cm^{-1}, 100 cm^{-1}, and 130 cm^{-1} from the central main band. Their relative intensities vary with matrix and temperature. The absorption at lowest energy is identical with one of the bands of the crystal of hydrogen chloride.[19] The second band of the crystal appears 225 cm^{-1} to lower energy from the central band.

D. DISCUSSION

The absorption bands of lithium fluoride in argon, krypton, and nitrogen matrices at 4.2K at 836 cm^{-1}, 841 cm^{-1}, 831 cm^{-1}, and 776 cm^{-1} have been reported and discussed by Linevsky.[14] This author assigns these absorptions to the diatomic monomer LiF and discusses the considerable shifts of the frequency as compared to the gas phase. Vidale[16] has reported the free molecule frequency as 900 cm^{-1}. The shifts have been analyzed by Linevsky in terms of the interactions between the LiF molecule and the surrounding matrix. The doubling of the band in the argon matrix has not received a satisfactory explanation, but the present work has only confirmed the earlier findings without adding to the interpretation.

The additional absorption bands observed here at 721 cm^{-1} and 717 cm^{-1} in the argon and krypton matrices respectively are here assigned to the LiF dimer. No corresponding absorption was observed so far for the nitrogen matrix. This band is expected to be shifted out of the sodium chloride region and will be investigated shortly. Klemperer and Norris have recently assigned absorptions at 640 cm^{-1} and 460 cm^{-1} to the LiF dimer.[17] The present results are not in agreement with this assignment since the gas phase frequency is expected to lie at higher energy compared to the matrix spectrum in analogy to the monomer spectrum behavior. As evidence for the assignment of the observed bands to the dimer, the results of experiments at different concentrations can be quoted. The rate of salt deposition was kept constant while the matrix flow rate was decreased by varying degrees, until a rate about ten times smaller than the band here assigned to the dimer was observed to gain appreciably on that of the monomer band.

As has been reported in the previous section, no absorption spectrum of cesium chloride was observed in the ultraviolet. This molecule is expected to absorb near 2500A at low temperature.[20] It is known from vapor phase studies[20] that the excited electronic states of all alkali halide molecules are very weakly bonding and their ultraviolet spectra are very diffuse. It is likely, therefore, that the absorptions are still more diffuse in the matrix and as a result could not be observed in our experiments.

The infrared absorption spectrum of hydrogen chloride in rare gas matrices has been described. In the limit of low concentration (1:1000) and low temperature (4.2K) a single narrow line is observed and this is assigned to the isolated molecule. At 20K this line is accompanied by two satellites, one 20 cm^{-1} to higher energy and the other 40 cm^{-1} to lower energy. This is the pattern to be expected for a rotating molecule since at this temperature the population in the J=L level is 70% of that in the J=0 state. The intensity ratios, as well as they can be

determined from the partly unresolved spectra, are in agreement with this interpretation. On raising the temperature of the solid solution the spectrum undergoes a series of changes until the known spectrum of the crystal appears. The intermediate spectra must be due to different stages of polymerization.

Acknowledgements: The work reported here was carried out by S. Schliek and M. Brith.

VIII. INVESTIGATION OF STRUCTURES OF METAL HALIDE AND METAL OXIDE SYSTEMS BY ELECTRON DIFFRACTION AND SPECTROSCOPIC TECHNIQUES*

A. BACKGROUND

Besides the inherent interest in the structures and other molecular constants of the metal oxide and metal halide vapors at elevated temperatures, there is at the present time a pressing need for their thermodynamic functions. The composition of such vapors can be determined from vaporization experiments (effusion, etc.), and the enthalpies for the evaporation or decomposition reaction may be obtained by the application of the second law. However, the measurement of the entropy increments and, in particular, the estimation of the absolute entropies of the large variety of species which are present under these circumstances are much more difficult tasks. The objective of this program is to determine essential molecular constants with sufficient precision to permit determination of the rotational entropies. Then, with the aid of rough spectral data and the utilization of empirical relations between interatomic distances and force constants, one can make sufficiently good estimates of the vibrational frequencies to allow one to estimate the vibrational entropies as well.

We plan to undertake electron diffraction investigations of the structures of some halides, oxides, and/or hydroxides of hafnium and zirconium in the vapor phase. Since these substances have low vapor pressures at room temperature, the structural studies will require the use of a high temperature sample source.

The work that we have done so far in modifying our electron diffraction apparatus for the study of samples maintained at high temperatures has already borne fruit. We have determined the structures of cesium chloride monomer, lithium chloride dimer, and copper nitrate and have looked at several hydroxides of the alkali metals and the boron oxide system.

Whereas the apparatus we have at our disposal is not the most suitable one for this type of investigation, it is good enough to permit a preliminary investigation of these structures. This is an essential step prior to making a precision study. This modification for high temperature studies of our original electron diffraction apparatus is described in the literature.[21] An additional electron diffraction apparatus for high temperature application has been designed and is under construction. Funds for its construction have been provided by sources other than this program.

Preliminary to the electron diffraction analysis, each of the compounds will have to be investigated mass spectrometrically to determine the composition of the vapor and to ascertain the concentrations of the species present in equilibrium with the solid or liquid phases. It is anticipated that such information will be already available for some of the substances to be considered.

---

* - Assembled from reports submitted by Professors S. H. Bauer and R. F. Porter, Cornell University, Ithaca, New York.

B. STATUS OF PROJECT

The possibility that the personnel required for this work might not be immediately available was anticipated in our original proposal. This proved to be the case. Dr. Kjell Hjortaas (Ph.D., structural chemistry, Oslo University) arrived in Ithaca in early October and has begun to assemble the required additional equipment and materials for electron diffraction investigations at high temperatures. Dr. Michio Kawano (Ph.D., molecular spectroscopy, Tokyo University) also began work at that time on the spectra of salts dissolved in nonionizing solvents. Dr. Kawano's salary is derived from sources other than this program.

The old diffraction camera is now being used by two other workers who began last spring to take data on the structures of N_2F_4 and $LiAlF_4$. In the meantime, Dr. Hjortaas has reactivated a high vacuum glass line, with ancillary equipment, for the preparation and degassing of metal salt and oxide samples. Also, he has designed a very fast pumping, all metal, vacuum system for such preparations. This is now being constructed in our shop.

Dr. Kawano surveyed the available literature on the solubilities of salts in a variety of nonaqueous solvents and selected anhydrous acetic acid as a solvent for the first tests. Raman spectra of 10% and 20% solutions of LiCl in $(HOAc)_2$ showed one new band and some interesting changes in the spectral shifts characteristic of the solvent. A Beckman IR-7 with a CsBr prism is now available for absorption spectra studies down to 40μ .

A major effort is being devoted to the completion of the new electron diffraction apparatus. The shop is making slow but steady progress. The major pieces have almost been completed. A somewhat optimistic estimate for completion is six months.

Our digital computer program for the computation of radial distribution functions and theoretical intensity curves is being improved and somewhat expanded.

C. FUTURE WORK

Only preliminary work has as yet been undertaken. We expect during the forthcoming year to:

1. Obtain electron diffraction data on the vapors of ZrF_4, $HfCl_4$, and HfF_4 and to establish their structures (it is our considered opinion that the structure of $ZrCl_4$ is now well enough established so as not to warrant further refinement at this time)

2. Pursue our current studies of the Raman and infrared absorption spectra of solutions of these salts in nonionizing solvents.

IX. THERMODYNAMIC PROPERTIES OF ZIRCONIUM AND HAFNIUM HALIDES*

One of the prime objectives of this phase of the program is an evaluation of various thermodynamic properties of the zirconium and hafnium halides through a study of the disproportionation equilibria of the type:

$2ZrCl_{3(c)} \longleftrightarrow ZrCl_{2(c)} + ZrCl_{4(g)}$; $ZrCl_{3(c)} \longleftrightarrow ZrCl_{3(g)}$; $ZrCl_{2(c)} \longleftrightarrow ZrCl_{2(g)}$.

It was proposed to study these equilibria by measuring the (equilibrium) pressure in a Knudsen cell containing the appropriate halides by the usual weight loss method and by a momentum measuring device, simultaneously. Combination of the resulting data in a manner analogous to that given by Searcy and Freeman[22] for the torsion-effusion method gives a value for the average molecular weight of the effusing species; if the various effusing species are known, the composition of the vapor can be calculated, and hence, equilibrium constants and heats of reaction.

The accomplishments to date have been achieved in two areas: development of a suitable momentum measuring device, and theoretical study of the correction factors for both total flow and angular distribution of molecules effusing from conical orifices. Each of these is discussed in some detail below.

A. ELECTRODYNAMOMETER

1. Introduction

One of the principal problems associated with studies of vaporization processes at high temperatures is identification of the vapor species. Margrave[23] has reviewed the techniques which have been used, and Gilles has recently pointed out in detail the difficulties associated with determination of the average molecular weight of effusing vapor by the torsion-effusion method.

We have for some years sought to develop a device capable of measuring with an accuracy better than ± 1.0 percent the momentum of a molecular beam emanating from a Knudsen cell in which the pressure might be 10^{-6} - 10^{-3} atm. If the molecular beam impinges on a target, a force is exerted which is directly related to the average momentum of the molecules in the beam; the problem then becomes one of measuring this extremely small force, or if the target is attached to a suspension wire, of a very small (0.1 - 0.001 dyne-cm) torque.

The design of the basic measuring device, which is described briefly below and, for an earlier version, in greater detail by Dawson[25], is based on an absolute

* Submitted by Dr. R. D. Freeman, Radiochemistry, Inc., Louisville, Kentucky and Oklahoma State University, Stillwater, Oklahoma.

electrodynamometer constructed many years ago by the National Bureau of Standards[26] for evaluation of the absolute ampere. Guthe obtained a precision of 10-20 ppm. The electrodynamometer described here is physically smaller by a factor of about 5 and operating currents are smaller by factors of 10 to 100; the achievable precision is correspondingly decreased. In the initial design of the electrodynamometer an operating precision of 0.1 percent was the goal and, as shown below, this goal has been closely approached.

2. General Description

The electrodynamometer consists of a cylindrical coil of wire of a single layer suspended within a larger fixed coil, also cylindrical and of a single layer, the ratio of the radius of each coil to its length being $1/\sqrt{3}$. When the two coils have this particular shape and their centers coincide, the expression for the torque, which in general is given by a series of terms, is simplified by the disappearance of all terms after the first and up to the seventh, and this and succeeding terms are usually extremely small if the suspended coil is small in comparison to the stationary coil[27].

If the axes of the two coils are at right angles, the torque is then expressed by the formula[26]:

$$T = \frac{2\pi r^2 N_1 N_2 I_1 I_2}{C} = G I_1 A I_2 \qquad (1)$$

in which r is the radius of the suspended coil, and N_1 and N_2 are the whole number of turns of wire on the fixed and suspended coils respectively. I_1 and I_2 are the currents, in electromagnetic units, passing through the fixed and suspended coils respectively; they may or may not be identically the same current. C is one half the diagonal of the fixed coil, $\sqrt{a^2+b^2}$, a being the radius of the fixed coil and $2b$ its length; as stated above $a/2b = 1/\sqrt{3}$, or $a/b = 2/\sqrt{3} = 1.154700$. $G = 2\pi N_1/C$ is the magnetic force at the center of the stationary coil, if unit current flows through it, and $A = \pi r^2 N_2$ is the sum of the areas of the several turns of the suspended coil.

The equation for the magnetic force at the center of the stationary coil was derived assuming that the current density is the same along the length of the coil, or that the coil is encased in a current sheet. It has been shown by Rosa[28] that the magnetic force calculated from a coil with windings of insulated wire is equivalent to a current sheet to within less than one part per million.

3. Stationary Coil

The large coil was turned from a four-inch tube of Plexiglas, with a wall thickness of 0.25 inch, which had previously been cured at 100C for three hours. The form was threaded, 44 threads per inch, to allow the winding to be as even as possible. Windings on the coil consisted of 150 turns of 0.0221-inch diameter, "Nyclad"-insulated, copper magnet wire. Coil diameters were measured with a precision micrometer, which could be read accurately to 0.0001 inch and which was

checked with gauge blocks which were accurate to 0.000005 inch. The outside diameter of the wound coil was measured on six different axial planes at each of five equi-spaced positions along the length, giving a total of thirty diameters. One thickness of wire was subtracted from the average outside diameter to give the pitch diameter. The pitch diameter determined by this procedure was 9.9931 ± 0.0010 cm.

The length of the coil was measured along eight lines parallel to the axis and spaced at 45° intervals around the circular cross section; measurements were made with a toolmakers' microscope which was accurate to $\pm$ 0.0001 inches when compared with precision gaugeblocks. The average coil length is 8.6545 ± 0.0010 cm. The value of the ratio a/b for this coil is therefore 1.1547 ± 0.0003 compared with the desired theoretical value 1.15470.

The constant G may now be evaluated:

$$G = 2\pi N_1/C = 2\pi N_1/\sqrt{a^2 + b^2} = 142.58 \qquad (2)$$

However, in the derivation of this equation it is assumed that the winding of the coil is perfectly regular. Rosa[28] has shown that the effect of even slightly irregular winding on the magnetic force at the center of a coil is appreciable in precise work and that the correction for the effect of irregular winding may be made by dividing the winding into a number of sections and calculating the contribution G_i from each section to the magnetic field at the center of the entire coil:

$$G_i = \frac{2\pi n_i}{x_i - x_{i+1}} \left\{ \frac{x_i}{(a^2 + x_i^2)^{\frac{1}{2}}} - \frac{x_{i+1}}{(a^2 + x_{i+1}^2)^{\frac{1}{2}}} \right\} \qquad (3)$$

when n_i is the number of turns of wire per section, x_i and x_{i+1} are the perpendicular distances of the edges of the section from the central plane of the coil. Then $x_i - x_{i+1}$ is the length of the i th section. Appropriate measurements were made on the stationary coil to permit calculation of the G_is. The sum of the G_is is G' = 142.57, and is the corrected value of G, for which equation (2) gives 142.59. The difference $(G - G') = \epsilon = 0.02$ amounts to 1 part in 7000 and is negligible for our purposes; however, these results may be summarized by rewriting equation (1) as

$$T = (G - \epsilon)\, I_1 A I_2 = G' I_1 A I_2; \quad \epsilon = 0.02 \qquad (4)$$

As previously stated, the axes of the movable coil and the stationary must be at right angles for the simplified expression for the torque to be valid. To assure that the axes are at right angles and in the same plane, one must either align the two coils coaxially and rotate the movable coil exactly 90°, or align the axes of the movable coil and the stationary coil perpendicular to one another in the horizontal plane. The adjustment mechanism will be described later. It is sufficient to note here that the movable coil was suspended by a fine wire which passed through a 0.125-inch hole in the top of the stationary coil. The hole was located in the exact center of the winding with the aid of a centering microscope, and its axis was coincident with a diameter of the coil.

To facilitate initial alignment of the two coils with their axes perpendicular, two 0.062-inch holes were drilled in the stationary coil, one at each end of the diameter which passes through the center of the stationary coil and which is perpendicular to the axis of the opening for the suspension wire. The 0.062-inch holes were plugged with Plexiglas sighting tubes which had an internal diameter of 0.010 inch. Details of the alignment will be described below.

The placing of holes in the stationary coil necessitated the displacement of wires around them. The actual displacement of the various wires is given in Table IX. The effect of this displacement of wires on the magnetic field at the center must be determined.

TABLE IX

WIRE DISPLACEMENT FOR HOLES IN STATIONARY COIL

Diameter of Hole Inch	Number of Wires Displaced	Displacement Inches	Direction of Displacement
0.125	1	0.062	Horizontal, left
0.125	1	0.062	Horizontal, right
0.125	1	0.040	Horizontal, left
0.125	1	0.040	Horizontal, right
0.125	1	0.018	Horizontal, left
0.125	1	0.018	Horizontal, right
0.125	2	0.0681	Radial
0.125	2	0.0454	Radial
0.125	2	0.0227	Radial
0.062	4	0.0454	Radial
0.062	4	0.0227	Radial

Rosa[28] has discussed the effect on H, the field strength at the center of the coil, of such displacements. For a radial displacement da of all the turns of the coil, $dH/H = -4\,da/7a$, where a is, as above, the radius of the coil. For the 0.125-inch hole, the displacement occurs for an average distance of 1.0 inch along the circumference of the coil, or 1.0/12.429 of one complete turn. Also, the center section of ten wires contributes 12.55/142.57 of the total field strength (from the G_1 Calculations) and each wire contributes, on the average, 0.1 of this, or 0.0088 of the total field. Therefore,

$$-\frac{dH}{H} = \frac{4}{7} \times 0.0088 \times \frac{1.0}{12.429} \quad \frac{2(0.0681 + 0.0454 + 0.0227)}{1.9671} = 5.6 \times 10^{-5}$$

Hence, the error, or distortion, produced in the field at the center of the coil by radial displacement of the six wires around the 0.125-inch hole is about 6 parts per hundred thousand. For the radial displacement of the wires about the two 0.062-inch hole,

$$-\frac{dH}{H} = \frac{4}{7} \times \frac{0.5}{12.429} \times 0.0088 \quad \frac{4(0.0454 + 0.0227)}{1.9671} = 2.8 \times 10^{-5}$$

For the horizontal displacement dx of one turn of wire at distance x from the central plane parallel to itself, Rosa gives

$$\frac{d H}{H} = - \frac{3x\, dx}{a^2 + x^2}$$

or, for displacement from x_1 to x_2,

$$\frac{\Delta H}{H} = - \frac{3}{2} \ln \frac{a^2 + x_2^2}{a^2 + x_1^2}$$

if $\Delta H/H$ is small. The wires with the greatest displacement are the two displaced 0.062-inch about the 0.125-inch hole, i.e., displaced from $x_1 = 0.0113$ to $x_2 = 0.0733$ inch. Again, these wires are displaced 1.0/12.429 of a total circumference and each contributes 0.0088 of the total field. Therefore, for one wire displaced as above,

$$\frac{\Delta H}{H} = - \frac{3}{2} \ln \left(\frac{4 + (0.073)^2}{4 + (0.011)^2} \right) \times \frac{1.0}{12.429} \times 0.0088 = 0.0000014 = 1.4 \times 10^{-6}$$

If it is assumed that the six wires about the 0.125-inch hole and the eight about the two 0.062-inch holes are all displaced horizontally by the amount of maximum displacement, one obtains for the upper limit of the error in H:

$$\frac{\Delta H}{H} = 1.4 \times 10^{-6} \times 14 = 19.6 \times 10^{-6} = 2.0 \times 10^{-5}$$

or two parts per hundred thousand.

The total error from both horizontal and radial displacements is the sum of the above errors,

$$\frac{\Delta H}{H} = (2.0 + 5.6 + 2.8) \times 10^{-5} = 10.4 \times 10^{-5}$$

or one part in ten thousand which is completely negligible for our purposes.

4. Movable Coil

The movable coil was machined from a one-inch Plexiglas rod, which had been cured at 100C for three hours. The small coil was also threaded, 44 threads per inch. The windings consisted of 30 turns of 0.0221-inch diameter, "Nyclad"-insulated, copper magnet wire. The pitch diameter and the length of the small coil were determined in the same manner as they were for the stationary coil and were found to be 1.9964 ± 0.0010 and 1.7287 ± 0.0010 cm, respectively. From these the ratio of diameter to length is 1.1549 ± 0.0010 compared to the theoretical value 1.15470 and the constant $A = \pi r^2 N_2$ has the value 93.91 ± 0.04.

5. Suspension System

The suspension system will not be described in detail here. Briefly, the stationary coil is mounted on a brass plate which sits on a Kinematic support, the superstructure of which carries a micrometer screw for precise and reproducible adjustment of the vertical position of the suspended coil, and a worm-gear device for precise adjustment of the angular orientation of the axis of the suspended coil in the horizontal plane. Leveling bulbs are incorporated in the plate on which the large coil is mounted and in the superstructure.

The suspension wire is typically 21 cm in length and for most of the measurements has been 0.00079-inch diameter tungsten wire. Fourteen-karat gold ribbon, 0.0035 x 0.00026 inch, has also been used. The wire is clamped between small brass plates; assembly of the wire and mounting clamps, etc., is accomplished in a jig which permits alignment within $\pm$0.001 inch of the wire with the axis of its support.

Mounted on the suspension system immediately below the lower end of the suspension wire and immediately above the upper end are small cubical mirrors: the lower one facilitates determination of the orientation of the suspended coil; the upper one is used to determine the angle through which the upper end of the torsion wire is rotated for the comparative measurements described below. The angles between the vertical faces of the upper mirror were measured by the method described by Guthe[26]; all four angles were found to be 90.00$\pm$0.02 degrees.

In the ends of both the movable and the stationary coil were placed plugs with 0.010-inch holes located precisely on the axis of the coil. Alignment of the two coils with axes perpendicular, was then accomplished by: (1) adjusting the movable coil until its axis was coincident with that of the stationary coil as indicated by alignment of the end-plug holes (described above) when viewed with a telescope, and then rotating the suspension system 90.00 degrees as measured with the cubical mirror; or (2) adjusting the movable coil so that its axis was initially perpendicular to that of the stationary coil as indicated by alignment of the holes in the end plugs of the movable coil with the holes in the "sides" of the stationary coil when viewed with a telescope. Measurement on a spectrometer table indicated that the angle between the longitudinal axis of the stationary coil as defined by the end-plug holes and the diameter defined by the "side" holes is 90.00$\pm$0.04 degrees.

6. Electrical Leads and Control Circuit

The leads to the movable coil must hinder its rotational movement as little as possible. Several lead arrangements have been tried; the only successful one has been to connect electrically the ends of the suspended coil to immediately adjacent binding posts through two freely suspended, catenary loops of 0.002 x 0.0002-inch copper ribbon. Similar arrangements have been used at the National Bureau of Standards[29] in high precision current measuring devices.

The control circuit for the coil currents is shown schematically in Figure 16. The output voltage of the transistorized voltage regulator is constant

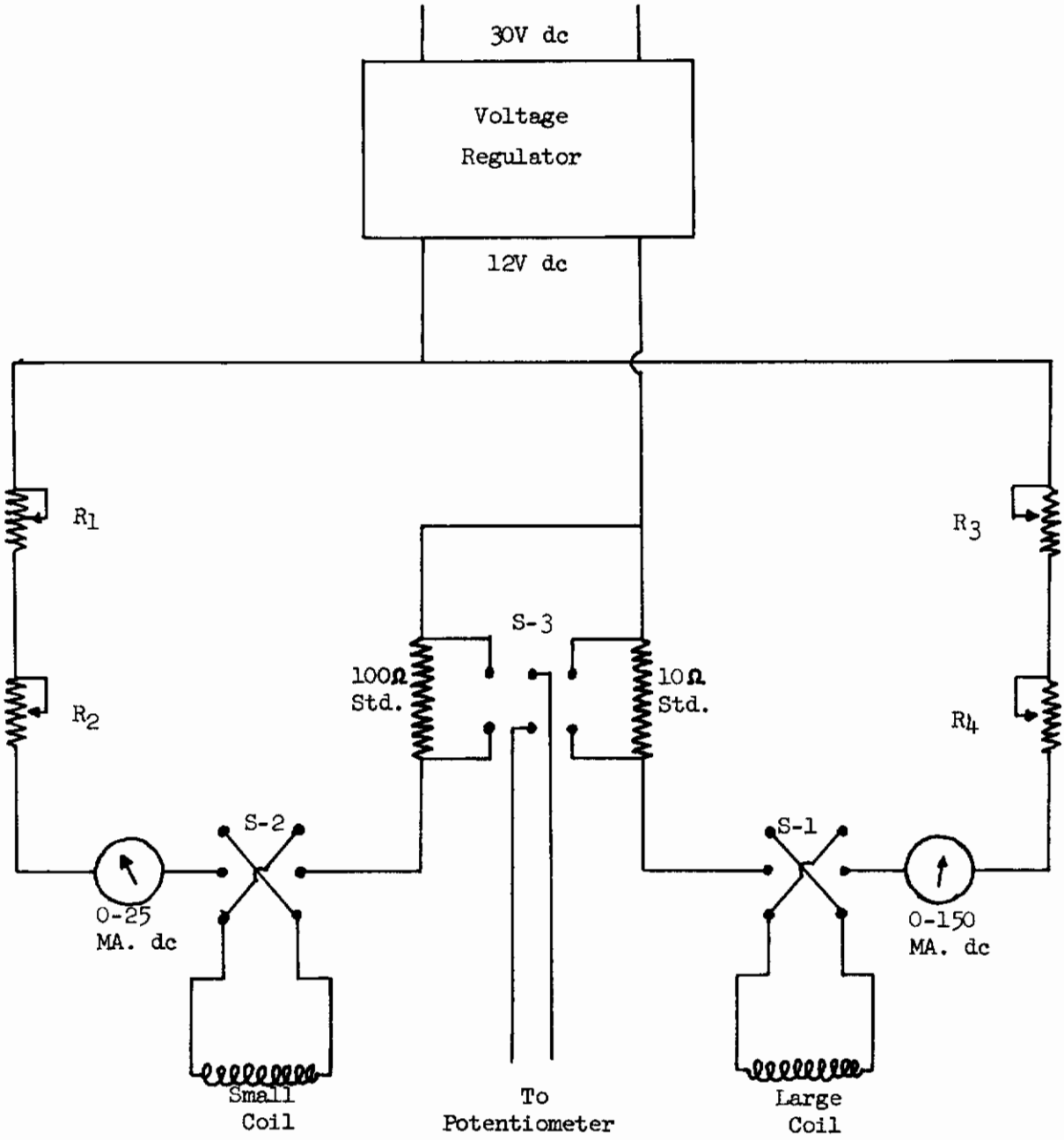

Figure 16. - Electrodynamometer Control Circuit

within less than ±0.1 percent over a several-hour period; the ripple voltage is 1 millivolt or less in the 12 v. output. Switches S-1, 2, and 3 are massive knife switches which reverse the direction of current in the coils and connect the potentiometer to the appropriate standard resistor.

7. Correction for Earth's Field and for Lead Wires

In Guthe's work[26] the two coils were connected in series so that identically the same current passed through both. Early in our work it became apparent that the current through the two coils would have to be controlled independently, because currents in the range 8 to 20 milliamperes through both coils can produce ambiguous results which arise from the comparable magnitude of the field of the large coil and the earth's field, and which are eliminated if the current in the fixed coil is sufficient to make the field of the fixed coil larger than the earth's field by a factor of at least 5.

For convenience equation (4) is written:

$$T = G'I_1AI_2 = giai' = Kii' \qquad (5)$$

with $G' = (2\pi N_1/C) - \epsilon = 10$ g; $A = \pi r^2 N_2 = 10$ a; $K = ga$; I_1 and I_2 in electromagnetic cgs units, and i and i' in amperes. The field strength H at the center of the large coil is $H = G'I_1 = gi$. The local horizontal component of the earth's field is represented by H_e; the effective horizontal component in oersted/10 units for combination with currents expressed in amperes is h_e, and $h_e = H_e \sin\Theta/10$, with Θ designating the angle between H_e and the axis of the suspended coil. The direction of h_e is chosen as positive; H may be parallel (+) or antiparallel (-), to h_e. The four possible combinations of flow of current in the coils are designated by j = 1, 2, 3, or 4; the positive direction of flow is arbitrarily chosen so that with both i_j and i'_j positive, H is positive and the resultant torque T_j is positive, i.e., upward by the right-hand rule. Table X gives these various relations in detail.

TABLE X

RELATIONSHIPS FOR THE FOUR POSSIBLE COMBINATIONS OF CURRENT FLOW

Direction* of Current, j	i_j	i'_j	H_e	T_j	Relative Magnitude of i'_j for Fixed T and i_j
1	+	+	+	+	low
2	-	-	-	+	high
3	+	-	+	-	low
4	-	+	-	-	high

*Corresponds to the four possible combinations of positions of the reversing switches of Figure 16.

Suppose that a negative torque is produced on the suspended coil by rotation of the upper end of the torsion wire and that this torque is exactly counterbalanced by a positive torque T_1 produced by coil currents for $j = 1$, i.e., i_1 and i'_1. If the currents are now reversed, $j = 2$, and the (same) negative torque again counterbalanced by positive torque T_2, the currents required, i_2 and i'_2, will be appreciably different from i_1 and i'_1. This difference may be attributed to the reversal of H with respect to the earth's field. Fields surrounding lead wires to the coil cannot contribute to this difference since the effect of these fields is the same in both magnitude and direction for $j = 1$ and $j = 2$. A similar argument is valid for the difference in currents, at constant torque, for $j = 3$ and $j = 4$. However, the currents measured for $j = 1$ and $j = 3$ differ in magnitude as well as direction, not because of the influence of the earth's field which is the same for both, but because any contribution to the torque from fields around lead wires is reversed in direction when the current in only one coil is reversed. This is also the case for $j = 2$ and $j = 4$. The contribution to the torque by lead wires is proportional to the product of the currents in the two coils and may be expressed as $\pm \delta i_j i'_j$, δ being the unknown, and hopefully small, positive proportionality constant.

Equations may now be written which describe the equilibrium counterbalanced situations discussed above and which explicitly describe the contribution from the earth's field and the lead wires:

$$T_j = Ki_j i'_j \pm \delta i_j i'_j + h_e a i'_j \qquad (6)$$

the negative sign being appropriate for $j = 3$ and 4 only. If equation (6) for $j = 1$ is multiplied by $-i'_2$, and that for $j = 2$ by i'_1, the resulting equations added and solved for $T_{12} = T_1 = T_2$, one obtains

$$T_{12} = (K + \delta) i^2_{12} = (K + \delta) i'_1 i'_2 (i_2 - i_1)/(i'_1 - i'_2) \qquad (7)$$

Similarly, from equation (6) for $j = 3$ and $j = 4$,

$$T_{34} = (K - \delta) i^2_{34} = (K - \delta) i'_3 i'_4 (i_3 - i_4)/(i'_4 - i'_3) \qquad (8)$$

It should be noted that this procedure has produced equations, (7) and (8), in which the contribution from the earth's field does not appear.

Equations (7) and (8) may combine in two ways to eliminate the contribution δ from the lead wires. First, if equations (7) and (8) are multiplied, and T_{12} and $-T_{34}$ $(=T_{12})$ are replaced by Tx, one may obtain

$$Tx = K(1 - \delta^2/K^2)^{\frac{1}{2}} (-i^2_{12} i^2_{34})^{\frac{1}{2}} \qquad (9)$$

Guthe[26] reported that $\delta/K = 1/12000$ for his apparatus; hence, the factor $(1 - \delta^2/K^2)^{\frac{1}{2}}$ contributed about 1 part in 3×10^8 and was dropped. Even if δ/K were as large as 1/10, the error introduced by omitting the factor $(1 - \delta^2/K^2)^{\frac{1}{2}}$ would be no greater than 0.5 percent; accordingly, this factor may be dropped and

$$T'_x = K(-i^2_{12} i^2_{34})^{\frac{1}{2}} \qquad (10)$$

Second, the contribution δ can be eliminated, rather than incorporated into a presumably negligible term, by multiplying equation (7) by i^2_{34}, equation (8) by i^2_{12}, and adding the resulting equations to obtain

$$T_z = T_{12} = -T_{34} = 2Ki^2_{12}i^2_{34}/(i^2_{34} - i^2_{12}) \tag{11}$$

A convenient check on the self-consistency of data resulting from the various directions of current flow may be obtained by equating equation (6) with $j = 1$ to (6) with $j = 2$, (T_1 and T_2 are required to be identical), from which one may obtain

$$\frac{h_e}{g} = (1 + \delta/K)(i_2i'_2 - i_1i'_1)/(i'_1 - i'_2) \tag{12}$$

Since h_e and g are constants determined by the earth's field and by the geometry and orientation of the fixed coil, the ratio h_e/g is an apparatus constant and the right side of equation (12) should be a constant regardless of individual values of i_j and i'_j or of the value of the torque being measured. The constant h_e/g is designated by ρ, and

$$\rho_{12} = (1 + \delta/K)(i_2i'_2 - i_1i'_1)/(i'_1 - i'_2) = (1 + \delta/K)\ R_{12} \tag{13}$$

An analogous equation may be obtained from equation (6) for $j = 3$ and $j = 4$:

$$\rho_{34} = (1 - \delta/K)(i_3i'_3 - i_4i'_4)/(i'_4 - i'_3) = (1 - \delta/K)\ R_{34} \tag{14}$$

It is convenient to write and use equations (7) through (14) in a form which considers only the magnitude of the torque and the currents; this transformation is easily made with use of Table X and yields:

$$T_{12} = (K + \delta)i^2_{12} \equiv (K + \delta)i'_1i'_2\ (i_1 + i_2)/(i'_1 + i'_2) \tag{15}$$

$$T_{34} = (K - \delta)i^2_{34} \equiv (K - \delta)i'_3i'_4\ (i_3 + i_4)/(i'_3 + i'_4) \tag{16}$$

$$T_x = K(1 - \delta^2/K^2)^{\frac{1}{2}}\ (i^2_{12}i^2_{34})^{\frac{1}{2}} \equiv K(1 - \delta^2/K^2)^{\frac{1}{2}}\ i^2_x \tag{17}$$

$$T'_x = K(i^2_{12}i^2_{34})^{\frac{1}{2}} \equiv K\ i^2_x \tag{18}$$

$$i^2_x \equiv (i^2_{12}i^2_{34})^{\frac{1}{2}} = i'_1i'_2i'_3i'_4\ (i_1 + i_2)(i_3 + i_4)/(i'_1+i'_2)(i'_3+i'_4) \tag{19}$$

$$T_z = 2\ K\ i^2_{12}i^2_{34}/(i^2_{12} + i^2_{34}) \equiv K\ i^2_z \tag{20}$$

$$\rho_{12} = (1 + \delta/K)(i_2i'_2 - i_1i'_1)/(i'_1 + i'_2) \equiv (1 + \delta/K)\ R_{12} \tag{21}$$

$$\rho_{34} = (1 - \delta/K)(i_4i'_4 - i_3i'_3)/(i'_3 + i'_4) \equiv (1 - \delta/K)\ R_{34} \tag{22}$$

From equations (17) and (20), if $T_x = T_z$

$$(\delta/K)^2 = 1 - (i^2_z/i^2_x)^2 \qquad (23)$$

and from equations (21) and (22), if ρ_{12} and ρ_{34} are required to be equal as they theoretically should,

$$\delta/K = (R_{34} - R_{12})/(R_{12} + R_{34}) \qquad (24)$$

8. Experimental

To check the combined accuracy of construction of the coils and of alignment procedures the torque produced by the rotation through $\pi/2$ radians of a calibrated suspension wire was measured with the electrodynamometer. After the coils had been aligned and the suspension calibrated as described below, the upper end of the torsion wire was rotated through $90.00 \pm 0.02^\circ$, as measured by the cubical mirror; the resulting torque on the small coil was exactly counterbalanced by the torque produced by currents through the two coils. The currents were measured by standard resistor and potentiometer as indicated in Figure 16. The currents were then reversed, the torque again counterbalanced, and the currents measured. These two sets of measurements are for directions $j = 1$ and $j = 2$. The upper end of the torsion wire was then rotated back through the null position which was checked for constancy, to a position $-\pi/2$ radians from null so as to produce on the small coil a torque equal in magnitude but opposite in direction to that produced by the initial rotation above. This torque was then counterbalanced by currents flowing in the two possible directions, $j = 3$ and $j = 4$.

The torsion constant, D, of a wire can be obtained by measuring the period of oscillation, t, when mass of known moment of inertia, I, is suspended by the wire: $D = 4\pi^2 I/t^2$. In the electrodynamometer suspension system, the lower wire clamps and mirror assembly remain in place for both calibration and measurement, and represent a moment of inertia I_x which is difficult to calculate precisely. This difficulty is eliminated by measuring the periods of oscillation, t_a and t_b, when masses with moments of inertia I_a and I_b are suspended; the torsion constant is then obtained by combining equations

$$D = 4\pi^2 (I_i + I_x)/t_i^2 \; ; \; i = a, b, \text{ to obtain}$$

$$D = 4\pi^2 (I_a - I_b)/(t_a^2 - t_b^2) \qquad (25)$$

Table XI gives the details of determination of the torsion constant of wire No. 3, which was tungsten, 0.00079 inch in diameter. Each determination of a period of oscillation is accomplished by timing ten periods with an electronic scaler set to count the pulses of 60 cycle line current. The period was determined with each of five solid right cylinders, the masses of which range from 12.9 to 14.3 gm. Cylinder 4 is made of aluminum; others are of brass. As indicated in Table XI-A the periods of oscillation are highly reproducible. Table XI-B gives the torsion constant D calculated from equation (25) with data for various combinations of cylinders. The torsion constant calculated for combinations

TABLE XI

DETERMINATION OF TORSION CONSTANT OF WIRE NO. 3

A

Cylinder No.	I $gm\text{-}cm^2$	No. of sets of 10 Periods Measured	t sec.	Max. Dev. / Avg. Dev.
1	2.7561	6	31.73 ± 0.01	3
2	3.1899	6	33.95 ± 0.02	2
3	5.8460	6	45.44 ± 0.01	1.5
4	7.0645	6	49.89 ± 0.01	1.5
5	7.1859	6	50.24 ± 0.01	1.1

B

Cylinder a	Cylinder b	Torsion Constant D dyne-cm./Radian
2	1	(0.1175)
3	1	0.1153
4	1	0.1148
5	1	0.1153
3	2	0.1150
4	2	0.1145
5	2	0.1150
4	3	(0.1134)
5	3	0.1152
5	4	(0.1365)

(2,1), (4,3), and (5,4) may be eliminated from further consideration because each member of these combinations has a moment of inertia and period so nearly the same as that of the other member of the combination that considerable loss of precision occurs when the differences indicated in equation (25) are taken. The other seven values of D are in good agreement; the selected value is 0.1150 ± 0.0002 dyne-cm/radian.

Details of the results of measurement with the electrodynamometer of the torque produced by rotation of wire No. 3 through $\pi/2$ radians are given in Table XII. From these data R_{12} and R_{34}, equations (21) and (22), were calculated; from them δ/K was calculated by equation (24). This method of calculating δ/K assumes that $\rho_{12} = \rho_{34}$ for a given set of measurements; therefore, the excellent agreement between values of ρ_{12} and ρ_{34} for each measurement, Table XIII, is expected and redundant. However, these quantities should have constant value for each set of measurements. As Table XIII shows, the values of $\rho_{12} = \rho_{34}$ are indeed constant within ± 0.2 percent for the six measurements.

Table XIII also gives the values of the torque calculated by equations (17), (18), and (20). The value of K is obtained from the data for the coils given above:

$$K = ga = G'A/100 = 142.57 \times 93.91/100 = 133.89$$

The torque exerted by the suspension wire when rotated $\pi/2$ radians from the null position is then:

$$T_w = D\Theta = 0.1150\ \pi/2 = 0.1806 \text{ dyne-cm}$$

9. Results

In Table XIV are summarized the results of comparisons, similar to those described above, of the torque generated by the electrodynamometer when known currents flow in the coils with the torque produced by rotation through a known angle of three calibrated tungsten torsion wires. Several points are to be noted in Table XIV: (1) all experimental quantities, with the exception of Θ (3,b) which was a preliminary run for small angles, are reproducible within a few tenths of a percent; (2) the apparatus constant D is quite reproducible for a given wire and reasonably constant with different wires; (3) the torques T_x, T'_x and T_z, calculated from equations (17), (18), and (20), are agreed within 0.1 percent, indicating that the lead wire interaction constant δ/K is small and essentially negligible for this apparatus.

The last column of Table XIV gives the final results of the comparisons: the ratio of the torque T_z generated by the electrodynamometer to the torque T_w produced by rotation of the calibrated wire. The results, especially those with wire No. 3 which had by far the most stable null position, would appear to indicate that the electrodynamometer is capable of measuring torques in the 0.01 to 0.2 dyne-cm range with a precision of ± 0.2 percent and an accuracy of ± 1.0 percent, and perhaps of ± 0.5 percent. In view of the difficulties usually encountered in obtaining stable, reproducible tungsten torsion wires of such small diameter, and of the

TABLE XII

CURRENTS THROUGH ELECTRODYNAMOMETER COILS TO COUNTERBALANCE TORQUE OF (0.1150 $\pi/2$) RADIANS

Expt. No.	Coil Current	Milliamperes Current Direction, j 1	2	3	4
I	i	100.74	100.66	100.98	100.90
	i'	12.107	15.190	12.038	15.111
II	i	100.93	100.83	100.83	100.76
	i'	12.095	15.166	12.041	15.122
III	i	100.62	100.51	100.66	100.56
	i'	12.121	15.215	12.055	15.146
IV	i	100.63	100.50	100.49	100.45
	i'	12.113	15.202	12.075	15.164
V	i	100.64	100.58	100.71	100.64
	i'	12.131	15.225	12.029	15.108
VI	i	100.64	100.56	100.54	100.48
	i'	12.149	15.240	12.038	15.114

TABLE XIII

TORQUE PRODUCED BY ELECTRODYNAMOMETER
WITH CURRENTS GIVEN BY TABLE XII

Expt.	δ/K	milliampere ρ_{12}	milliampere ρ_{34}	(milliampere)^2 i_x^2	(milliampere)^2 i_z^2	dyne-cm T'_x	dyne-cm T_x	dyne-cm T_z
I	0.0024	11.36	11.36	1354.7	1354.7	0.18138	0.18138	0.18138
II	0.0036	11.36	11.36	1354.4	1354.4	0.18134	0.18134	0.18134
III	0.0026	11.36	11.36	1353.7	1353.7	0.18125	0.18125	0.18125
IV	0.0028	11.34	11.34	1353.3	1353.3	0.18119	0.18119	0.18119
V	0.0019	11.37	11.37	1353.4	1353.4	0.18121	0.18121	0.18121
VI	0.0019	11.33	11.33	1353.6	1353.6	0.18123	0.18123	0.18123
Average		11.35	11.35			0.18127	0.18127	0.18127

TABLE XIV

COMPARISON OF TORQUES

MEASURED BY ELECTRODYNAMOMETER AND BY ROTATION OF WIRE

Wire No.	Torsion Constant, D dyne-cm / radian	Angle of Rotation θ radians	milliamps	Torque, dyne-cm: Wire $T_w=D\theta$	Torque, dyne-cm: Calculated from Currents T'_x	Torque, dyne-cm: Calculated from Currents T_x	Torque, dyne-cm: Calculated from Currents T_z	T_z/T_w
1	0.1087 ±3z2*	1.5708 ±3z4	11.08 ±1z2	0.1707 ±3z2	0.1688 ±3z3	0.1688 ±3z3	0.1687 ±3z3*	0.988
2	0.1052 ±3z3	1.5708 ±3z4	11.27 ±1z1	0.1652 ±3z3	0.1667 ±3z2	0.1667 ±3z2	0.1667 ±3z2	1.009
3a	0.1150 ±3z2	1.5708 ±3z4	11.35 ±1z1	0.1806 ±3z2	0.1813 ±3z1	0.1813 ±3z1	0.1813 ±3z1	1.004
3b	0.1150 ±3z2	0.1230 ±2z2	11.26 ±1z5	0.01415 ±3z2	0.01418 ±4z1	0.01418 ±4z1	0.01416 ±4z1	(1.002)

* - All errors given are average deviations of experimental values, not absolute errors; N ±3z4 = N ±0.0004.

fact that the torsion wire is of necessity calibrated under dynamic conditions and used under static ones[30], it may well be that a carefully constructed electrodynamometer is more nearly accurate for measuring small static torques than is the usual calibrated torsion wire.

The correlation of torques measured by rotation of torsion wires and by the electrodynamometer will continue until the quality of performance of the electrodynamometer is reasonably well established. The apparatus will then be employed in the disproportionation reactions discussed earlier.

B. MOLECULAR FLOW

1. Introduction

Molecular flow is defined as the flow of gas molecules at pressures sufficiently low that the mean free paths are much longer than the dimensions of the containing vessel. The large majority (90-95 percent) of the collisions which the molecules undergo are with the walls.

If two reservoirs containing gases at molecular-flow pressures are separated by a thin wall and an orifice is cut in this wall, gas molecules will begin to flow between the reservoirs. If the pressures in the reservoirs are constant, the rate of flow through the orifice in either direction is determined only by the dimensions of the orifice. If the wall thickness is very small, i.e., the length of the orifice is negligible with respect to its radius, the rate of flow is determined only by the area of the orifice. If, however, the wall has appreciable thickness, the rate of flow will be decreased because some molecules upon striking the wall of the orifice will be returned to the reservoir from which they came.

The fraction of molecules which, having entered an orifice, pass through without being returned to the reservoir from which they came is called the transmission probability of the orifice, or the "Clausing factor" after a pioneer in the field of molecular flow. These theoretical factors for cylindrical orifices have been considered by many workers, most recently by DeMarcus[31] and Carlson[32], and are known with high precision, and if the initial assumptions are correct with high accuracy. In theoretical analyses of molecular flow[33,34,31,32] it has been generally assumed that a molecule striking an inert surface at a point will eventually be "reflected" from the same point. It has been further assumed that the probability of the molecule being "reflected" at a given angle from the normal to the surface at the point of "reflection" is proportional to the cosine of that angle, i.e., diffuse reflection occurs, not specular reflection. It has never been shown with reasonable certainty that these assumptions are indeed valid for molecular flow through orifices.

It is often desirable to use tapered orifices in effusion measurements at high temperatures. A theoretical treatment of molecular flow through tapered, or conical, orifices was recently given by Balson[35] but is nonrigorous.

Use of devices which measure the momentum of a molecular beam, e.g., the torsion-effusion apparatus, or the electrodynamometer device described above,

requires knowledge of the angular distribution of molecules within the beam. For ideal orifices, with infinitesimal length, the distribution follows the well-known cosine law. For cylindrical orifices Clausing[33] and Freeman and Searcy[36] give appropriate theoretical correction factors; for tapered orifices no distribution functions or data are available.

This section of the report describes briefly the derivation and calculation of theoretical transmission probabilities and angular distribution functions for conical orifices. These derivations and computations will be described in detail after the computations, now in progress, are completed.

2. The Conical Orifice

We consider a region composed of the (inside) walls of an orifice of length L and its entrance (0) and exit (L) faces. For convenience we will arbitrarily consider the entrance face to be to the left, the exit to the right. The symbol n with appropriate subscripts represents the number of molecules which, per unit area per second, pass through an imaginary planar area or impinge on a wall within the region. This number will be constant over the entire region if the pressures outside the entrance and exit faces are constant and equal. If these pressures are constant but unequal, $n_{(0)}$ will be constant over the entrance face, $n_{(L)}$ will be constant over the exit face, but n_x, the incident density on the walls, will vary with the distance $x(0 \leqslant x \leqslant L)$ from the entrance face.

The transmission probability W of the orifice may now be defined by

$$W = \frac{N_L}{N_0} = \frac{\int_{\text{region}} nP(z)dA}{\int_{(0)\text{face}} n_{(0)}\,dA} \qquad (1)$$

N_0 is therefore the number of molecules which enter (the (0)face of) the orifice per second and N_L, the number which leave the exit (L) face per second; P(z) is the probability that a molecule emanating from an incremental area dA with generalized coordinates z will pass directly through the exit (L) face. The denominator of equation (1) may be easily evaluated from elementary kinetic theory if the pressure on the (0) face is known and constant, which we shall assume. It is the numerator of equation (1) which presents difficulties.

The integral in the numerator can be split into integrals over the entrance face and over the walls:

$$N_L = \int_{(0)\text{face}} n_{(0)}P(z)dA + \int_{\text{walls}} n_x P(z)dA \qquad (2)$$

The first integral in equation (2) is easily evaluated since $n_{(0)}$ is known and constant and P(z) can be evaluated from geometrical considerations and the cosine law. The second integral presents difficulties because n_x varies with x in a complicated way.

To evaluate n_x, the incident density on the walls, we note that molecules arriving at a point on the wall at x come from three areas: the entrance face, the exit face, and other points on the walls. Thus, one can write

$$n_x = \int_{(0)\text{face}} n_{(0)} P(A;x)dA + \int_{(L)\text{face}} n_{(L)} P(A;x)dA + \int_{\text{walls}} n_x P(A;x)dA \qquad (3)$$

in which $P(a;x)dA_x$ is the probability that a molecule emanating from the area dA will impinge in the area dA_x at x. These probability functions can again be determined from geometrical considerations, and $n_{(0)}$ and $n_{(L)}$ are known and constant; the first and second integrals of equation (3) may therefore be readily evaluated. However, the third integral necessarily contains the function n for which the equation was supposed to provide a solution.

Equation (3) is of the type

$$f(x) = g(x) + \int_a^b K(x,y)f(y)dy$$

which is well known to mathematicians as a Volterra-Fredholm integral equation. Solutions are guaranteed for f if g is bounded and $0 \leqslant K \leqslant 1$ on $a \leqslant y \leqslant b$. The methods for obtaining solutions are usually numerical and tedious. DeMarcus[31] has obtained an elegant, relatively simple solution if the kernel K(x,y) is of the displacement type $K(x,y) = K(|y-x|)$, i.e., the kernel depends only on the distance between x and y and not on the separate variables. This latter restriction is applicable to cylindrical orifices but not conical orifices.

Our solution of equation (3), and therefore of equation (1), for the conical orifice has proceeded to the point at which all the necessary probability functions have been evaluated, a method for solving integral equation (3) with a high-speed computer has been proposed, the corresponding computer program written, and plans have been made for using a computer at W-PAFB to obtain the solutions. These will be described in detail later.

X. KINETICS OF REACTION BETWEEN FLUORINE AND REFRACTORY BORIDES AND CARBIDES*

A. INTRODUCTION

The powerful oxidizing property of fluorine finds potential applications both in industry and rocket technology. This has revived the interest in the study of fluorine chemistry and kinetics of reactions between fluorine and other materials. Earlier studies have largely been confined to the search for suitable materials to handle fluorine. Therefore, quantitative data relating to the kinetics and mechanism of reaction involving fluorine and refractory materials are desired at this time.

B. PREVIOUS WORK

Extensive work on the mechanism of corrosion of metals by oxygen or air has been done but very little work has been reported for other gases, including fluorine. Leech[37] and Slesser and Schram[38] have reported that copper and nickel can be used for handling elementary fluorine. The first kinetic study involving fluorine was made by Brown et al [39]. They found that the reaction between fluorine and copper followed a logarithmic growth law suggested by Evans[39], but were unable to explain the observed variation in activation energy for the reaction with increasing film thickness.

Jarry et al[40] reported at an American Chemical Society meeting their study on the fluorine-nickel reaction at 700C and fluorine-zirconium reaction over the temperature range 300 to 500C. However, they have not yet published any quantitative data. They concluded that reaction proceeds by the migration of fluorine through the fluoride film to the nickel-film interface.

M. O'Donnell et al[41] studied the fluorine-copper reaction extensively from 800 to 1200F at a pressure of 200 mm of pressure. They found that the reaction was diffusion controlled and obeyed a power law rate equation of the form $y^n = kt$ in the temperature range of 800 to 1000F. At higher temperatures a logarithmic rate law was the best for the observed data. For very long periods of time the experimental data were best described by an asymptotic law, $y = K(1 - e^{at})$ for all temperatures studied.

C. EXPERIMENTAL DETAILS AND APPARATUS

The thermogravimetric method will be used to follow the course of fluorination reactions. The experimental set-up is shown in Figure 17.

---

* - Submitted by Dr. T. C. M. Pillay, postdoctoral fellow, and Professor John L. Margrave, project director, University of Wisconsin, Madison, Wisconsin.

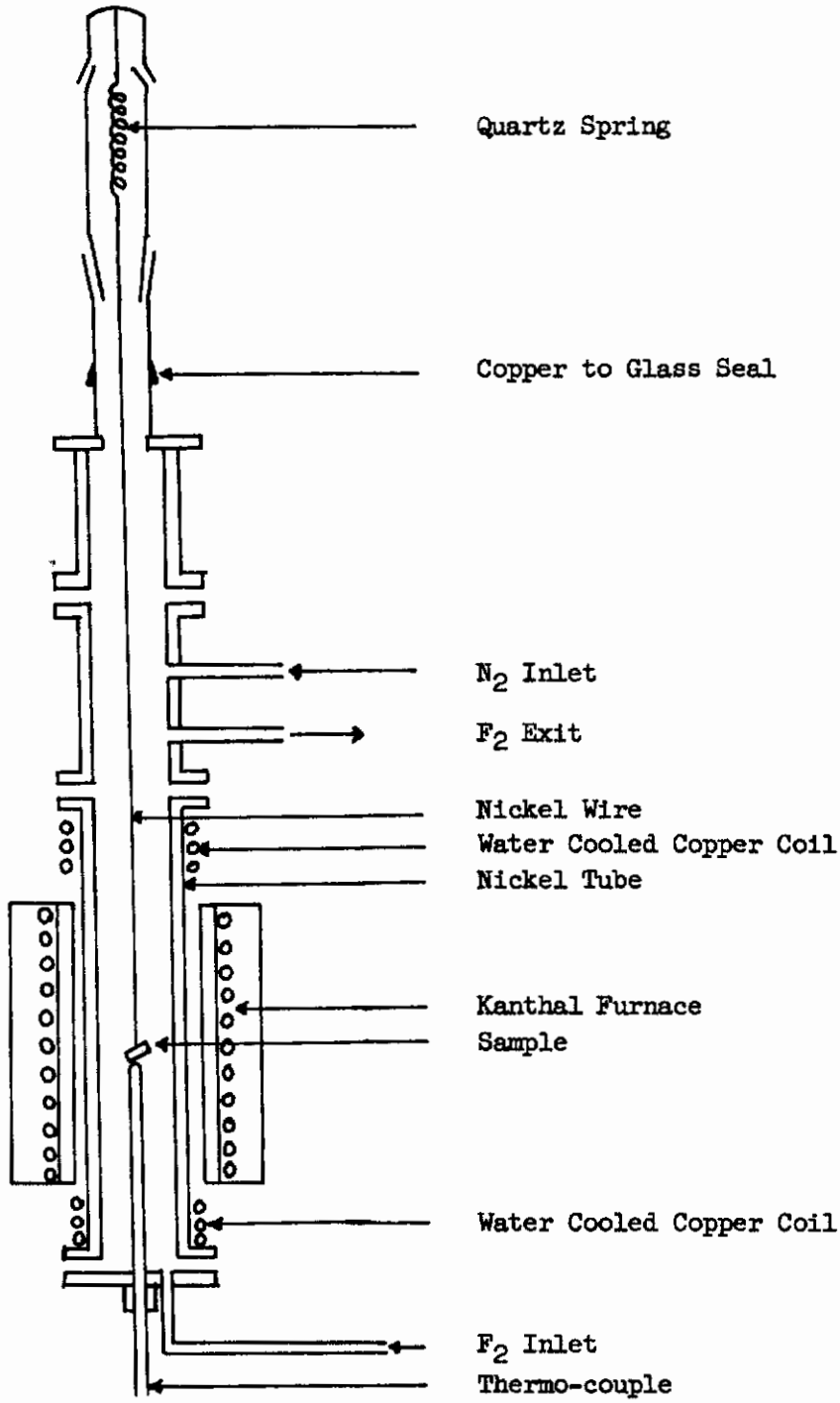

Figure 17. - Furnace and Gravimetric Apparatus for Fluorination Kinetics

The reaction chamber consists of a nickel tube 12 inches x 1.0 inches I.D. and 1/8 inch wall thickness. The heating is done by a Kanthal wound resistance furnace capable of operation up to 1250C. The temperature is maintained steady by a controller and measured by a properly insulated chromel-alumel thermocouple introduced from the bottom flange of the furnace through a nickel tube of 1/4 inch I.D., closed at the top end.

The sample is suspended from the helical quartz spring into the hot zone of the furnace by a fine nickel wire. The weight changes of the sample determine the extension of the spring which is read on a cathetometer. The spring has a maximum load capacity of 2.0 gm and has a sensitivity of 9.902 mg per 1 mm of extension.

The flow of fluorine gas is regulated by nickel Hoke valves and metered by a Fisher-Porter glass rotameter containing a sapphire float. The fluorine is blocked from entering into the glass case containing the quartz spring by a regulated flow of pure nitrogen. The fluorine is drawn out from the top of the furnace through two columns of activated alumina.

The apparatus is being calibrated by studying the oxidation of zirconium in the temperature range of 400 - 1200C. Cubiciotti[42] has reported a parabolic rate for zirconium oxidation in the temperature range of 600 - 900C. Culbransen and Andrew[43] also have established a parabolic rate law for oxidation of zirconium in the temperature range of 400 - 800C.

D. FUTURE WORK

The mechanism of corrosion of high-purity borides and carbides of hafnium and zirconium by fluorine will be investigated. Samples of high-purity ZrB_2 are now available. Further studies on HfC, ZrC, HfB_2, etc., with O_2, F_2, H_2O and mixtures are planned as samples are available.

XI. MASS TRANSPORT STUDIES*

A. INTRODUCTION

It has been observed that the corrosion rates of metals in various atmospheres are frequently dependent on the rate at which one of the reacting species can move through the tarnishing layer. For oxidation, the tarnishing films are metal oxides and, after the initial reaction, further oxidation must proceed via a mechanism of mass transport through the oxide layer. In a perfect ideal lattice in which an atom is located on every lattice site there would be no ionic mobility and thus no mass transport. In real materials, however, there are always present, owing to composition or to thermal energy, vacant lattice sites or interstitial ions which contribute to ionic mobility. Measured ion mobilities depend on the number of these defect sites (fixed by composition and temperature) and on the energetics of this motion. Other postulated mechanisms not involving a defect lattice, such as place exchange, can be shown to be energetically very improbable as a means for ionic or atomic movement. Mass transport in the solid is thus dependent on the defect structure which in turn is determined by temperature, stoichiometry, and impurity content of the material.

The initial reaction of zirconium and hafnium carbides and borides in oxidizing atmospheres will result in the formation of a thin oxide layer on the surface. Subsequent oxidation may depend on the rate of transport through this layer. Thus, mass transport through the zirconium or hafnium oxides (or nitrides in the case of nitrogen atmospheres) can be an important process in the over-all reaction kinetics of the carbides and borides with oxygen (or nitrogen) containing atmospheres. A fundamental investigation of mass transport mechanism is essential to a better understanding of reaction kinetics in these systems. By suitable modifications of stoichiometry or impurity concentrations it may be possible to inhibit mass transport by several means: (1) by raising the energy requirements for defect formation, (2) by reduction in the number of available vacancy sites, and (3) by raising the activation energy of the mobile species.

B. BACKGROUND

Previous work on mass transport in zirconium oxides has dealt almost exclusively with solid solutions of ZrO_2 with V_2O_3, MgO, CaO, In_2O_3, and other valent impurities. Pure ZrO_2 exists in two crystalline structures: a monoclinic form, stable to about 1150C, and a more dense tetragonal modification which is the stable form above this temperature. The addition of the above-mentioned lower valent oxides promotes the formation of a cubic crystal lattice which is stable throughout the temperature range. The inclusion of these lower valent metals favors the formation of oxygen vacancies in the ionic lattice. The observed increase in electrical conductivity (indicative of increased ion transport) of these mixed systems can be explained in terms of the formation of these vacancies. As further confirmation of this type of activated conduction process, the temperature coefficient for conductivity is negative and thermoelectric power measurements on these mixed

* - Prepared by Dr. H. Michael Klein, Arthur D. Little, Inc., San Francisco, Calif.

systems indicate positive charge carriers. There is no work reported in the literature on mass transport in pure ZrO_2 or in mixed systems with higher valent impurities.

Since the electrical conduction process must be related to the motion of charges in the material it seems appropriate to investigate electrical conductivity as a means of providing information on oxygen transport in zirconium oxide. Conductivity (σ) in solids is often found to obey the empirical relationship

$$\sigma = Ke^{-E/kT}$$

and thus a plot of ln σ vs. 1/T will yield the activation energy for the conduction process. The variation of conductivity with impurity concentration should yield information on the number of lattice defects and combined with the conductance-temperature data the energetics of lattice defect formation can be obtained as well as individual ion mobilities.

In our studies it may prove necessary to determine and separate any electronic contributions to the total conductivity. This can be done by a transference number experiment after the method of Tubandt. Disks of ZrO_2 are pressed together and electrolyzed for a known time with a known dc current.[2] In analogy to the classic electrolytic solution case, the anode, cathode, and middle compartments are separated and weighed. Any weight changes can be directly related to the transference numbers of the ionic species.

In aqueous solutions and in alkali halide crystals where electrical conduction is due to ionic mobility, electrical conductivity and transport number are related to the diffusion coefficient and absolute mobility by the Nernst-Einstein equations:

$$D_i = \kappa_i kT$$

$$\sigma_i = n_i Z_i^2 e^2 \kappa_i = \sigma t_i$$

D_i = diffusion coefficient
κ_i = ionic mobility
σ = total conductivity
n_i = concentration
Z_i = valence
e = electronic charge
T = absolute temperature
t_i = transference number

Thus, conductivity studies can provide information on oxygen self-diffusion. However, conductivity studies will be limited by temperature due to electrical lead and connection problems. It is planned to supplement the conductivity work with oxygen self-diffusion studies which will permit comparison between methods and extension of the mass transport studies to high temperatures.

The experimental method will be to plate one end of the sample with O^{18} enriched ZrO_2, equilibrate it at temperature for a known time, section it, reduce the sections[2] with carbon in an effusion cell, and analyze mass spectrometrically the effusion gases for O^{18} and thus determine the concentration gradient. The solution of Fick's Second Law for these boundary conditions is of the form $C = C_0(\pi Dt)^{1/2}e^{-x^2/4Dt}$. Plots of log C vs. X^2 will give the required diffusion constants.

C. EXPERIMENTAL WORK

To date, the experimental effort has been directed toward sample preparation and the development and construction of equipment for the diffusion and conductivity work.

The major components for a versatile conductance bridge capable of an accuracy of about 0.05% have been ordered and received, and construction and testing are in progress. Also, vacuum equipment necessary for the diffusion studies and for the conductivity work in various atmospheres has been purchased. A high vacuum line is currently being assembled. Funds for this equipment have been provided from sources other than this contract.

For the experimental samples, we have been trying to obtain zirconium dioxide single crystals. Previous work has dealt exclusively with pressed powders and sintered specimens. We feel, however, that a careful study of a well-characterized sample will be of much greater value in understanding the conduction and diffusion process. Measurements made on sintered materials in which porosity and grain boundary effects may introduce significant uncertainties seem to have little merit for describing the transport mechanism in this oxide and determining the effect of stoichiometry, structure, and impurity content on mass transport.

Single crystals of quartz, sapphire, zinc oxide, V_2O_3, and several other oxides have been grown by the use of basic aqueous solvents at high pressure and temperature which increases the solubility of these ordinarily insoluble materials. This technique of hydrothermal synthesis has proved quite successful in growing relatively large single crystals of these amphoteric oxides which are comparatively strain free since they are made at moderate temperatures and are not subject to the excessive temperature gradients characteristic of flame fusion and melting techniques.

Since zirconium dioxide undergoes a sharp phase transformation tetragonal⟶ monoclinic at about 1150C on cooling from elevated temperatures, hydrothermal synthesis offers one of the few feasible approaches for growing ZrO_2 single crystals. In view of the fact that there is no information in the literature on the ZrO_2-H_2O system or ZrO_2 - (Na_2O; Na_2CO_3; NaOH) - H_2O system, our initial experiments have been exploratory in nature and based principally on the advice of other investigators in the field who have had success with hydrothermal synthesis for other oxide systems. We have performed a few experiments in an attempt to detect solubility of ZrO_2 in pure H_2O, 1M NaOH, 1M Na_2CO_3, and .5M H_2SOH at temperatures to 435C and pressures to about 35,000 lbs/in^2. No solubility was evident under these conditions. Since in many amphoteric systems the hydroxide is more soluble than the oxide, some tests were made in the above solvent systems and under the same supercritical conditions using zirconium hydroxide (precipitated with ammonia from a sulfate solution) as the nutrient. No solubility could be detected here either. We are currently obtaining noble metal liners so that the apparatus can be used to high pressures and temperatures with more corrosive solvent systems.

Since we have no interest in involving ourselves in long-term crystal synthesis programs we have been considering other alternatives which might provide valid data without the need for ZrO_2 single crystals. These alternatives include the use of other oxide crystals for mass transport studies to establish the effects of stoichiometry, structure, and impurity content or the development of alternate measurement techniques which may be applied to polycrystalline ZrO_2 and permit the separation of interfacial and bulk properties.

XII. REFERENCE CITATIONS

1. E. F. Westrum, Jr., J. B. Hatcher, and D. W. Osborne, J. Chem. Phys., 21, 419 (1953).

2. D. W. Osborne and E. F. Westrum, Jr., J. Chem. Phys., 21, 1884 (1953).

3. B. H. Justice, "Calculation of Heat Capacities and Derived Thermodynamic Functions from Thermal Data with an IBM 704 Digital Computer," U. S. Atomic Energy Commission Report TID-6206, June 1960; revised and modified in the Appendix to "Thermodynamic Properties and Electronic Energy Levels of Eight Rare Earth Sesquioxides," Doctoral Dissertation, University of Michigan, 1961.

4. Quoted in Thermodynamic and Kinetic Studies for a Refractory Materials Program, Second Semiannual Progress Report to Wright-Patterson Air Force Base, by L. A. McClaine, Program Manager, Wright Air Development Division, No. C-63081, July 1961. (See also corresponding sections of this report: Section III by G. Feick and Section V by J. L. Margrave.)

5. J. L. Margrave, personal communication.

6. Cf. K. K. Kelley, "Contributions to the Data on Theoretical Metallurgy. XIII.", Bureau of Mines Bulletin 584, Washington, D. C., 1960, p. 6.

7. R. T. Grimley, Ph.D. Thesis, University of Wisconsin, 1957.

8. Under study by Dr. Ward Hubbard at Argonne National Laboratory.

9. D. R. Stull and G. C. Sinke,"Thermodynamic Properties of the Elements," Adv. in Chem., 18, Am. Chem. Soc. (Washington 1956).

10. G. W. Otvos and D. P. Stevenson, J. Am. Chem. Soc., 78, 546 (1956).

11. F. W. Glaser and B. Post, Trans. AIME, 197, 1117 (1953).

12. J. M. Leitnaker, Los Alamos Scientific Laboratory Report LA-2402 (1960).

13. E. Whittle, D. A. Dows and G. C. Pimentel, J. Chem. Phys., 22, 1943 (1954) I. Norman and G. Porter, Nature, 174, 508 (1954).

14. M. J. Linevsky, J. Chem. Phys., 34, 587 (1961).

15. W. Klemperer, W. G. Norris and A. Buchler, J. Chem. Phys., 33, 1534 (1960) S. A. Rice and W. Klemperer, J. Chem. Phys., 27, 573 (1957).

16. G. Vidale, J. Phys. Chem., 64, 314 (1960).

17. W. Klemperer and W. G. Norris, J. Chem. Phys., 34, 1071 (1961).

18. R. Miller and P. Kusch, J. Chem. Phys., 25, 860 (1956)
J. Berkowitz and W. A. Chupka, J. Chem. Phys., 29, 653 (1958).

19. D. F. Hornig and W. E. Osberg, J. Chem. Phys., 23, 662 (1955).

20. R. S. Milliken, Phys. Rev., 51, 310 (1937)
R. F. Barrow and A. D. Caunk, Proc. Roy. Soc., A219, 120 (1953).

21. S. H. Bauer, Tadashi Ino, and R. F. Porter, J. Chem. Phys., 33, 685 (1960).

22. A. W. Searcy and R. D. Freeman, J. Am. Chem. Soc., 76, 5229 (1954).

23. J. L. Margrave, in Physico-Chemical Measurements at High Temperatures, (Bockris, et al, editors) Butterworths, London (1959).

24. P. W. Gillis, Ann. Rev. Phys. Chem., 12, 431 (1961).

25. J. P. Dawson, M. S. Thesis, Oklahoma State University (1959).

26. K. E. Guthe, Bull. N.B.S., 2, 33 (1906).

27. G. W. Patterson, Phys. Rev., 20, 300 (1905).

28. E. B. Rosa, Bull. N.B.S., 2, 71 (1906).

29. R. L. Driscoll, J. Res. N.B.S., 60, 287 (1958).

30. J. A. Bearden, Phys. Rev., 56, 1023 (1939).

31. W. C. DeMarcus, K-1302, parts 1-6, Union Carbide and Chemical Corp., Oak Ridge, Tenn.

32. K. D. Carlson, ANL 6156, Argonne National Laboratory, Lemont, Illinois (1960).

33. P. Clausing, Z. Physik, 66, 471 (1930).

34. P. Clausing, Ann. Physik, 12, 961 (1932).

35. E. W. Balson, J. Phys. Chem., 65, 1151 (1961).

36. R. D. Freeman and A. W. Searcy, J. Chem. Phys. 22, 762 (1954).